

Dobrogeria aegyssensis, a new early Spathian (Early Triassic) coelacanth from North Dobrogea (Romania)

LIONEL CAVIN¹ AND EUGEN GRĂDINARU²

¹Department of Geology and Palaeontology, Natural History Museum, CP 6434, 1211 Geneva 6, Switzerland.
E-mail: lionel.cavin@ville-ge.ch

²Department of Geology, Faculty of Geology and Geophysics, University of Bucharest, Blvd. Bălcescu Nicolae 1, RO-010041 Bucharest, Romania.
E-mail: egradin@geo.edu.ro

ABSTRACT:

Cavin, L. and Grădinaru, E. 2014. *Dobrogeria aegyssensis*, a new early Spathian (Early Triassic) coelacanth from North Dobrogea (Romania). *Acta Geologica Polonica*, **64** (2), 161–187. Warszawa.

The Early Triassic witnessed the highest taxic diversity of coelacanths (or Actinistia), a clade with a single living genus today. This peak of diversity is accentuated here with the description of a new coelacanth discovered in the lower Spathian (Upper Olenekian, Lower Triassic) cropping out in the Tulcea Veche (Old Tulcea) promontory, in the city of Tulcea, in North Dobrogea, Romania. The bone remains were preserved in a block of limestone, which was chemically dissolved. The resulting 3D and matrix-free ossifications correspond mostly to elements of the skull and branchial apparatus. Posterior parietals, postparietal with associated prootic and basisphenoid allow a precise description of the neurocranium. Ossifications of the lower jaw, together with branchial and pectoral elements, complete the description of this coelacanth and support the coining of a new generic and specific name, *Dobrogeria aegyssensis*. A phylogenetic analysis of actinistians with the new species recovers clades which were found in most recent analyses, i.e. the Sasseniidae, the Laugiidae, the Coelacanthiformes, the Latimerioidei, the Mawsoniidae and the Latimeriidae, and identifies the new taxon as a non-latimerioid coelacanthiform.

Key words: Actinistia; Latimeriidae; Triassic; Braincase; New taxon; Skull.

INTRODUCTION

The coelacanth *Dobrogeria aegyssensis* sp. nov., described herein, comes from the lower Spathian (Upper Olenekian, Lower Triassic) of the North Dobrogean Orogen. This orogen is a Cimmerian fold-and-thrust belt, located in the foreland of the Alpine Carpathian Orogen (e.g. Săndulescu 1995), and represents the westernmost segment of the Palaeotethyan Cimmerian orogenic system (Text-fig. 1A; see Şengör 1984). The puzzling position of the North Dobrogean Tethyan-type Triassic in the foreland of the Carpathian Orogen can be hypothetically argued as the result of the post-Triassic large scale horizontal displacements of Tethyan terranes in close connection with the open-

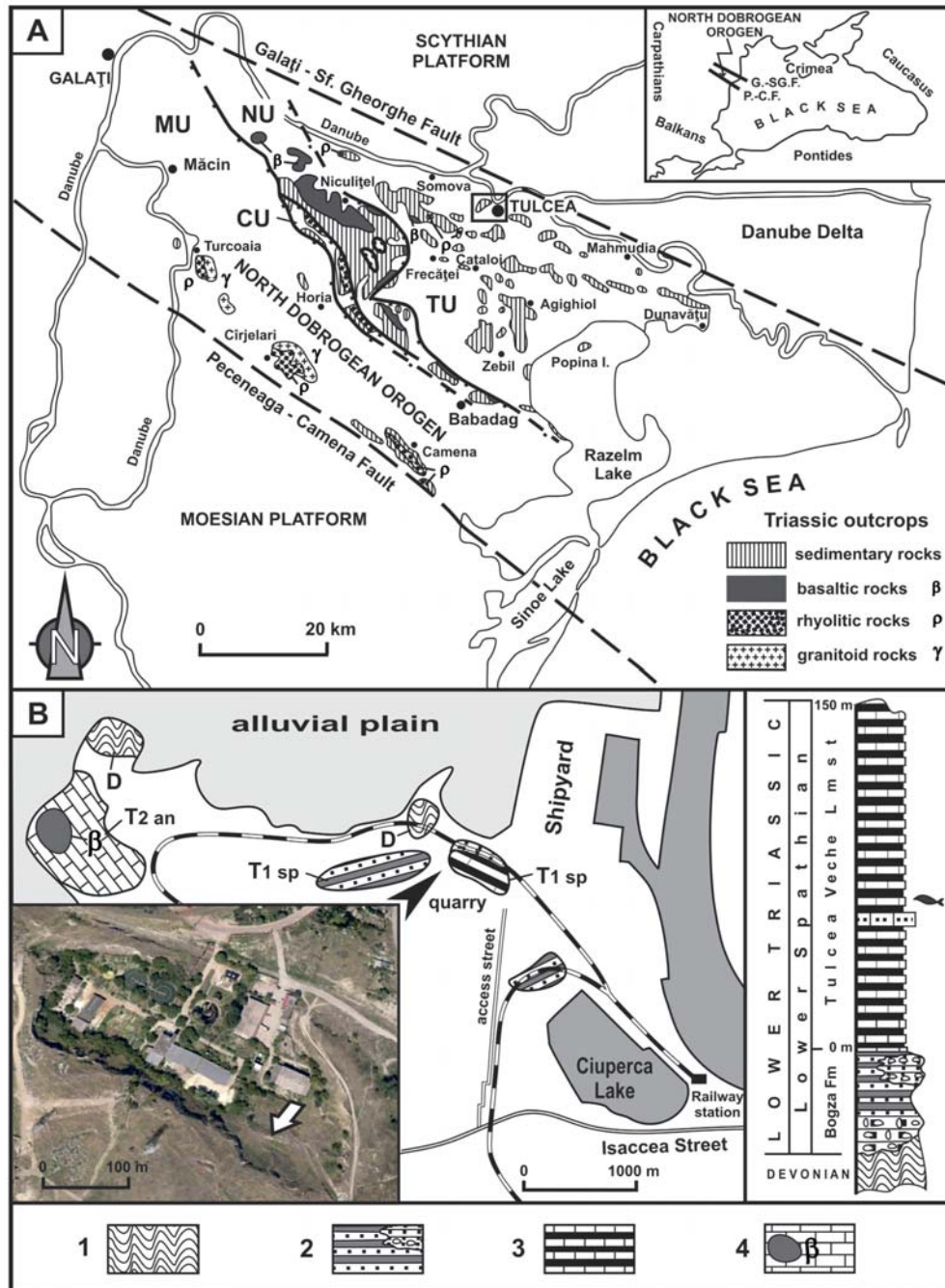
ing of the West Black Sea basin (Grădinaru 1995, 2000, 2006).

Triassic sedimentary rocks are present in all tectonic units of the North Dobrogean Orogen, which is a pile of north-easterly verging thrust-sheets or nappes (Text-fig. 1A). The Triassic sedimentary rocks have the largest development in the Tulcea Unit, with basal facies in its western-inner part, and with a carbonate platform in its mid-eastern part. The Triassic of the Tulcea Unit is well-known for its richness in various groups of Tethyan-type fossils (Kittl 1908; Simionescu 1913b; Grădinaru 2000).

In spite of over a century of studies of the Triassic of the North Dobrogean Orogen, only a few marine vertebrates have been found and described (Simionescu

1913a), all of them from the Tulcea Unit. The fieldwork carried out during the last decades in the region by one of us (EG) resulted in the discovery of new vertebrate material, which suggests much higher potential of the unit for further vertebrate finds. The present paper reports on the coelacanth fish from the lower Spathian (Upper Olenekian, Lower Triassic).

The actinistians, or coelacanth, are sarcopterygian fishes that first appeared in the fossil record in the Early Devonian (Johanson *et al.* 2006). The clade shows a relatively high morphological disparity in the Devonian (Friedman and Coates 2006), then an evolutionary conservatism until the present. The taxic diversity of the group was proportionally never high,



Text-fig. 1. A – Geological sketch map of the North Dobrogean Orogen: MU – Măcin Unit; CU – Consul Unit; NU – Niculițel Unit; TU – Tulcea Unit. Inset map shows location of the North Dobrogean Orogen (after Grădinaru 2000, modified). Box shows the type locality. B – Geological map of the Tulcea Veche (Old Tulcea) Promontory. 1 – Devonian (D); 2 & 3 – Lower Spathian (T1_{sp}), terrigenous sequence (2), limestone and marly shale (3); 4 – Middle Triassic, Anisian (T2_{an}), massive limestone with basalt intrusion (β). Inset with Google Earth image of the Tulcea Veche quarry, the arrow showing the fossil site of *Dobrogeria aegyssensis* gen. et sp. nov.

with the highest peak probably corresponding to a radiation event following the Permo–Triassic mass extinction in the Early Triassic (Cloutier 1991; Forey 1998; Schultze 2004; Wen *et al.* 2013; Cavin *et al.* 2013).

LOCALITY AND STRATIGRAPHIC DATA

The type locality of the newly described coelacanth is in a long-abandoned quarry (Google Earth coordinates: 45°11'28" N; 28°46'40" E; elev. 18 m), located on the Tulcea Veche (Old Tulcea) promontory (Text-fig. 1B, inset Google Earth image). The Variscan basement, made up of Devonian quartzites and calcschists, is disconformably overlain by Early Triassic sedimentary rocks (Mirăuță 1966). The Triassic succession (Text-fig. 1B, inset stratigraphic column) starts with thick-bedded matrix-supported conglomerates with quartz clasts and coarse-grained quartzose sandstones grading upwards or interfingering with medium to thick-bedded sandstones interbedded with reddish clay shales. The fully marine deposition started with a carbonate sequence known as the Tulcea Veche Limestone. The sequence is composed of thinly-bedded dark greyish micritic limestones interbedded with dark black, bituminous marly shales, with sporadic thin beds of fine-grained bioclastic limestones. The absence of trace fossils and the high content of organic matter indicate an anoxic to dysoxic depositional environment for the sequence. The first data on the fossil content and the age of this carbonate sequence were given by Simionescu (1908, 1911), who compared the sequence to the “Werfener Schichten”. The early Spathian age of the Tulcea Veche Limestone is well documented by a newly collected ammonoid fauna including *Tirolites cassianus* Hauer, *T. haueri* Mojsisovics, *Dinarites mahomedanus* Mojsisovics, and bivalves, such as *Leptochondria alberti* (Goldfuss), *Eumorphotis venetiana* (Hauer), and *Crittendenia decidens* (Bittner). In the quarry, the early Spathian carbonate sequence is highly tectonized by block faulting, accompanying the Galați-Sf. Gheorghe fault. The coelacanth material described herein was found as disarticulated bones, but not dispersed, in a block of limestone.

REPOSITORY

The material is housed in the Naturhistorisches Museum Wien, Department of Geology and Paleontology, to which it was donated by the second author (EG) of the present paper.

Institutional abbreviations: NHMW, Naturhistorisches Museum Wien, Austria.

MATERIAL AND METHODS

The studied material was chemically prepared by dissolving the bone-bearing limestone block with 10 % diluted glacial acetic acid. When the acid dissolution was completed, the samples were gently rinsed and the mud around the bones was carefully removed. If necessary, the fragile or crushed bones were impregnated with glue. This operation was repeated until the bones were fully extracted from the hard rock. The extracted bones are three-dimensionally preserved. If not damaged during the extraction or crushed by rock deformation, the coelacanth material is very well preserved, indicating that the anoxic/dysoxic environment precluded the destruction of the bone by scavengers. From the dissolved limestone block, measuring 40 × 30 × 8 cm, more than 50 fully preserved bones were extracted, and many other broken bones, including ribs, ray fragments, teeth and scales were also recovered. Several ossifications fit together and obviously belong to a single specimen, together with other bones, whose sizes indicate that they probably belong to the same specimen. However, supernumerary ossifications such as a posterior parietal, a quadrate and several angulars, generally smaller in size than the ossifications referred to the main individual, indicate the occurrence of at least another individual, smaller in size and less complete. Ossifications belonging to the larger individual, identified as such either because bones fit together or because bone size are compatible, are catalogued under the number NHMW 2013/0609 ranging from NHMW 2013/0609/0001 to NHMW 2013/0609/0035, and ossifications belonging to the smaller individual are catalogued under the number NHMW 2013/0610, ranging from NHMW 2013/0610/0001 to NHMW 2013/0610/0014. We cannot exclude the possibility that some of the isolated ossifications, especially those from the smaller individual, might belong to several different individuals. The studied material is listed in Appendix 1.

A parsimony analysis was run in PAUP* 4.0b10 (Swofford 2001) in order to explore the phylogenetic relationships of Actinistia with the inclusion of the new taxon. A heuristic search (using random addition sequence, replicate 100 times, 1 tree held at each iteration, and tree bisection and reconnection branch swapping) was carried out to try to avoid the tree ‘islands’ problem (Maddison 1991).

SYSTEMATIC PALAEOLOGY

Class Osteichthyes Huxley, 1880
 Subclass Sarcopterygii Romer, 1955
 Infraclass Actinistia Cope, 1871
 Order Coelacanthiformes Huxley, 1861 sensu Forey,
 1998
 Family Incertae Sedis

Genus *Dobrogeria* gen. nov.

TYPE SPECIES: *Dobrogeria aegyssensis* sp. nov.

ETYMOLOGY: From Dobrogea, the Romanian province situated between the lower Danube River and the Black Sea.

DIAGNOSIS: As for the type species, by monotypy.

Dobrogeria aegyssensis sp. nov.
 (Text-figs 2–15)

ETYMOLOGY: From Aegyssus, the ancient Greek settlement once occupying the site of the city of Tulcea.

HOLOTYPE: NHMW 2013/0609, isolated skull ossifications (posterior parietal, postparietal, prootic, basisphenoid, palatoquadrate, angular, splenial, gular plates, branchial elements), which are referable to a single individual.

TYPE HORIZON: Lower Spathian, beds with *Tirolites cassianus*.

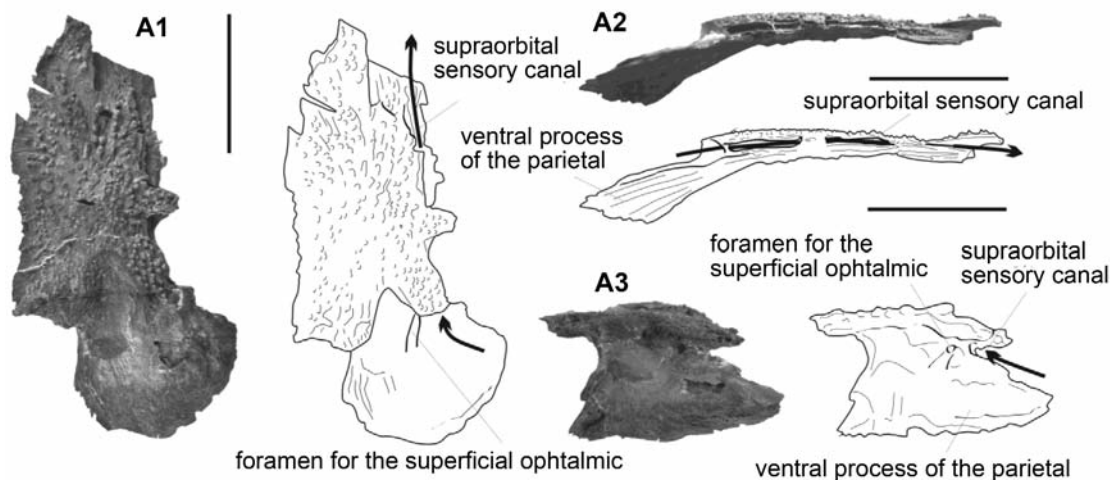
TYPE LOCALITY: Tulcea Veche (Old Tulcea) promontory, Tulcea city, North Dobrogea (Romania).

OTHER MATERIAL: NHMW 2013/0610. Isolated skull ossifications of smaller individuals found within the same block of limestone as the holotype.

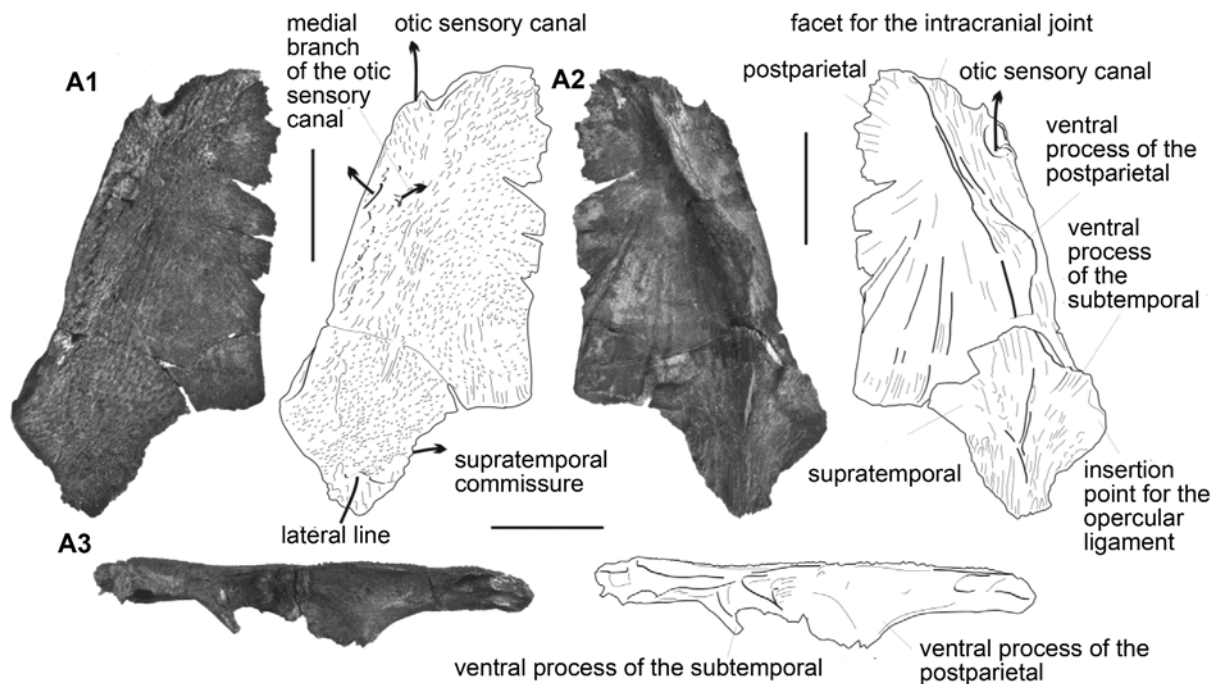
DIAGNOSIS: Coelacanthiform with a descending process on the postparietal; anteriorly expanded lachrymo-jugal; skull roof flat and ornamented with tubercles; posterior margin of the horizontal lamina of the posterior parietal deeply notched and extending posteriorly by a ca 25° inclined fan-shaped ventral process; postparietal shield approximately as long as wide and with a deep posterior embayment to receive the extrascapulars, which were not sutured to the skull roof; gular plates broad, approximately three times longer than wide; opercle right triangle in shape.

DESCRIPTION

Skull roof: Two right posterior parietals, forming part of the skull roof of the parietonasal shield, are undoubtedly identified. The most complete (NHMW 2013/0609/0001, Text-figs 2 and 7) matches an isolated basisphenoid found associated (Text-fig. 4), and probably belongs to the same individual. The posterior parietal is formed by a horizontal ornamented lamina, which was a part of the skull roof, and by the ventral process. The horizontal lamina bears a coarse ornamentation consisting of radiating lines of tubercles. The lateral and medial borders are approximately parallel. Although damaged, the anterior margin appears to have tapered, but we cannot exclude that the anterior margin was almost straight. Moreover, because an overlap usually occurs between the anterior and posterior parietals in coelacanth, the preserved margin may not correspond to the visible margin on the articulated skull roof. The posterior margin of the posterior parietal forms a deep notch. Its other margins, extremely thin and incompletely preserved in some of its portions, indicate that interdigitated sutures were probably present medially with the opposite parietal and laterally with the supraorbitals. The ventral process of the parietal, which was regarded as a separate ossification by several authors (see Forey 1998, pp. 44–46 for a discussion), forms a fan-shaped smooth blade of bone ventrally inclined at ca 25° from the horizontal lamina and with a regular convex posterior border. The supraorbital sensory canal, partly preserved, is present along the lateral margin of the horizontal lamina. It is preserved as a groove along some parts of its course and as a bone-enclosed canal on other. This arrangement indicates that the path of the sensory canal straddled the suture between the parietal and the supraorbital series as in other coelacanth except *Miguashaia* (Forey, 1998). A short canal, which opens medially to the sensory canal at the limit between the horizontal lamina and the ventral process, and extending on the ventral process as a groove, accommodated the superficial ophthalmic nerve. There are thus separate openings for the sensory canal and for the ophthalmic nerve, contrary to *Macropoma lewesiensis*, for instance, in which the nerve penetrates directly within the sensory canal (Forey 1998, fig. 82). In *Macropoma*, moreover, the ventral process is L-shaped in dorsal view (Forey 1998, fig. 3.19), unlike the shape of the material described herein. In *Laugia groenlandica*, the horizontal lamina of the parietal is without ornamentation and the foramen for the superficial ophthalmic nerve opens ventrally to the opening of the sensory canal (Forey 1998, fig. 3.8). In *Spermatodus pustulosus*, the posterior mar-



Text-fig. 2. Photographs and semi-interpretative line drawings of the right posterior parietal of the actinistian fish *Dobrogeria aegyssensis* gen. et sp. nov., NHMW 2013/0609/0001 (holotype) in dorsal (A1), lateral (A2) and posterior (A3) views; Tulcea Veche Limestone, Lower Spathian, Tulcea. Scale bars: 20 mm



Text-fig. 3. Photographs and semi-interpretative line drawings of left half of the skull roof of the postparietal shield of the actinistian fish *Dobrogeria aegyssensis* gen. et sp. nov., NHMW 2013/0609/0002 (holotype) in dorsal (A1), ventral (A2) and lateral (A3) views; Tulcea Veche Limestone, Lower Spathian, Tulcea. Scale bars: 20 mm

gin of the parietal is also dug by a notch, but the ventral process differs in its roughly triangular shape and in the occurrence of a strong ridge (Forey 1998, fig. 3.12).

A smaller right posterior parietal (NHMW 2013/0610/0001), with only the horizontal lamina preserved, shows tubercular ornamentation, whose pattern differs from the larger posterior parietal by being not arranged in lines.

From the skull roof of the postparietal shield, one right and one left postparietal, obviously belonging to

the same large individual (NHMW 2013/0609/0002 and NHMW 2013/0609/0003) are preserved, still sutured to their corresponding supratemporals (Text-figs 3 and 7). The external surface of the postparietal is ornamented with granulation arranged in ridges radiating from the centre of ossification. The general shape of the bone is proportionally long, ca twice longer than wide at its anterior part, and the bone broadens slightly posteriorly. The posterolateral margin, which sutures with the supratemporal, is slightly concave, while the medial half of the posterior margin forms, to-

gether with the posteromedial margin of the supratemporal a regularly curved margin against which abutted the extrascapulars. There is no trace of a sutural surface along this margin, indicating that the extrascapulars were probably free from the skull roof. The articulatory facet for the intracranial joint of the skull roof, very faint, is best observed in ventral view (Text-fig. 3 A2). It is located almost in the mid-width of the anterior margin. On the ventral side of the postparietal runs a strong crest along the anterior third of the ossification, which developed as the ventral process of the postparietal at about its mid-length.

The ornamentation of the supratemporal is similar to the ornamentation of the postparietal, making difficult the recognition of the suture between both ossifications. The supratemporal is lozenge-shaped (Text-fig. 3). On its ventral side, a rectangular shallow process located at the lateral corner of the bone marks the insertion point for the opercular ligament. Medial to the process the descending process of the supratemporal forms a shallow crest continuing the postparietal crest (Text-fig. 3 A3). The ventral process of the postparietal and the ventral process of the supratemporal match two corresponding processes present on an associated isolated prootic (see below).

The otic sensory canal runs within the supratemporal and the postparietal. It divides within the former to give off a medial small pore for the supratemporal commissure, and a much larger pore for the lateral line at the posterior corner of the supratemporal (Text-fig. 3 A1). In the postparietal, some laterally oriented pores are visible along the lateral margin of the bone. The canal opens anteriorly via a large rounded pore located on the ventral side of the ossification. On the right and left postparietals, a few pores are present medially to the path of the otic canal at the anterior third of the length of the bone, which suggests the presence of a short medial branch of the otic sensory canal. A pore is also visible dorsally, in a notch of the anterior margin of the bone.

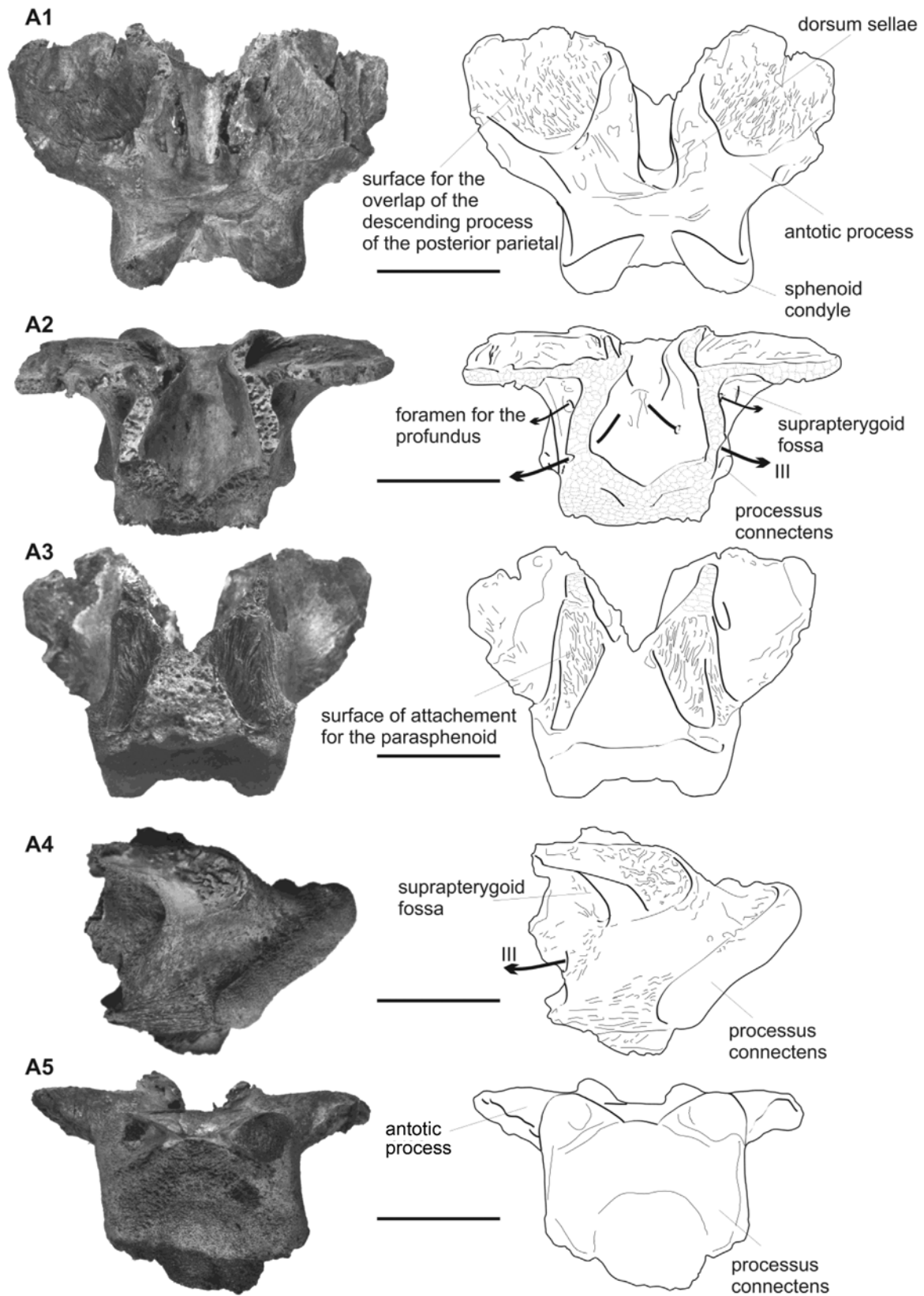
Compared with other coelacanth for which the postparietal shield are known, our specimen shows a general pattern more similar to *Holophagus*, *Macropoma* and *Latimeria* (Forey 1998), because of the presence of descending processes on both the postparietal and the supratemporal. *Laugia* is similar in its general outline, but the ventral side of the postparietal bears only a crest with no ventral process.

The posterior margin of the posterior parietal and the anterior margin of the postparietal have deep notches indicating that the intracranial joint margin was strongly interdigitate.

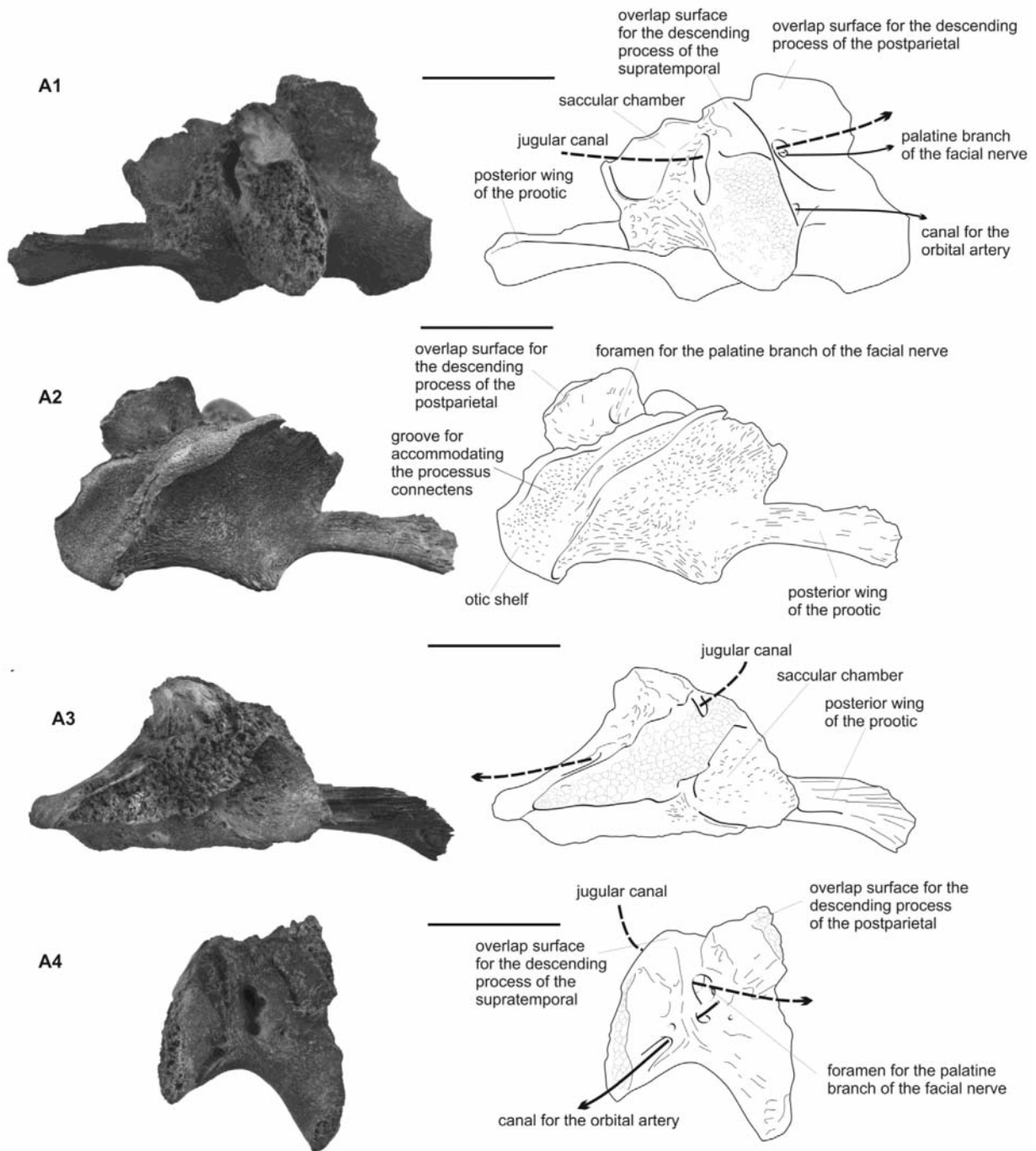
Braincase: Isolated bones from both the ethmo-

sphenoid and parietonasal portions are preserved, most of them belonging probably to the same specimen. From the ethmosphenoid shield, only a well preserved basisphenoid was recovered (NHMW 2013/0609/0004, Text-figs 4 and 6). The sphenoid condyles are squarish in shape in dorsal view and protrude more than in *Macropoma* (Forey 1998). The antotic processes are proportionally very large, more laterally expanded than in *Macropoma*, and show a large overlapping surface for the descending processes of the posterior parietals. The processus connectens are elongated, with parallel margins, and are in contact ventrally with the parasphenoid. The foramen for the profundus opens in the bottom of the suprapterygoid fossa, and the foramen for the oculomotor nerve opens anteromedially, not at the same level on both sides of the ossification. Because of the good state of preservation of the specimen, this asymmetry is probably real and not caused by distortion. There is no trace of a suprapterygoid process on the neurocranium (Forey 1998, p. 193) and a basiptyergoid process is absent. Basisphenoids are strongly ossified bones in actinistians, commonly preserved in 3D, and several studies have compared basisphenoids between different taxa (Schaeffer and Gregory 1961; Schaumberg 1978; Forey *et al.* 1985; Forey 1998). The basisphenoid of *Dobrogeria* compares better with the third morphological type as defined by Schaeffer and Gregory (1961), i.e. basisphenoids with nearly rectangular antotic processes and with an extensive overlap area for the ventral lamina of the posterior parietal (the "pleurosphenoid" of Schaeffer and Gregory (1961)). This type is found in *Spermatodus*, *Moenkopia* and *Latimeria*.

From the otoccipital portion of the neurocranium, prootics, a basioccipital and catazygals are known. Both prootics of a single individual are preserved (NHMW 2013/0609/0005 and NHMW 2013/0609/0006, Text-figs 5 and 7). The otic shelf is short and its internal face is crossed by an inclined groove to accommodate the processus connectens of the basisphenoid. The dorsal edge of the prootic passed into cartilage and the contact with the skull roof was not complete. In between the prootic, postparietal and supratemporal was a gap, through which exited the otic ramus of the facial nerve (Text-fig. 7). The overlap surface for the descending process of the postparietal, or prefacial eminence, is proportionally elongated and shows a perfect match with the descending process of a postparietal described above. The overlap surface for the descending process of the supratemporal is small. The jugular canal is completely enclosed in bone, and opens posteriorly in an elongated foramen. A small foramen pierces medially the base of the prefacial eminence and extends as a



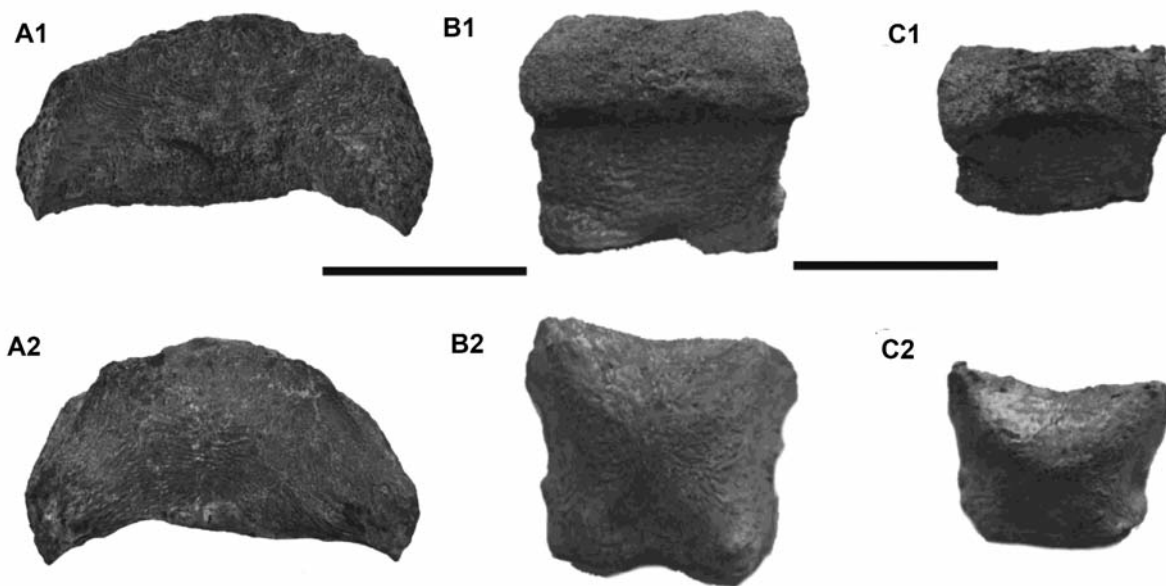
Text-fig. 4. Photographs and semi-interpretative line drawings of basisphenoid of the actinistian fish *Dobrogeria aegyssensis* gen. et sp. nov., NHMW 2013/0609/0004 (holotype) in dorsal (A1), anterior (A2), ventral (A3), lateral (A4) and posterior (A5) views; Tulcea Veche Limestone, Lower Spathian, Tulcea. Scale bars: 20 mm



Text-fig. 5. Photographs and semi-interpretative line drawings of the right prootic of the actinistian fish *Dobrogeria aegyssensis* gen. et sp. nov., NHMW 2013/0609/0005 (holotype) in lateral (A1), medial (A2), dorsal (A3) and anterior (A4) views; Tulcea Veche Limestone, Lower Spathian, Tulcea. Scale bars: 20 mm

canal which opens on the internal wall of the jugular canal, probably for the palatine branch of the facial nerve. The canal for the orbital artery opens in the bottom of the jugular canal and exits anterolaterally, beneath the overlap with the supratemporal. The course of the arteries and nerves differs from those in the la-

timeriids *Latimeria*, *Macropoma* (Forey 1998) and mawsoniid (Cavin and Forey 2004), but this structure appears to be quite variable among coelacanths (Dutel *et al.* 2012). Posteriorly the prootic is inflated and forms the wall of the saccular chamber. The posterior wing of the prootic is elongated and bears an enlarged extrem-



Text-fig. 6. Photographs of the basioccipital, NHMW 2013/0609/0007 (A), anterior anazygal, NHMW 2013/0609/0008 (B) and posterior anazygal, NHMW 2013/0609/0009 (C) of the actinistian fish *Dobrogeria aegyssensis* gen. et sp. nov. (holotype) in dorsal (1) and ventral (2) views; Tulcea Veche Limestone, Lower Spathian, Tulcea. Scale bars: 20 mm

ity with an interdigitated margin for the suture with the basioccipital. Smaller prootics (NHMW 2013/0610/0008 and NHMW 2013/0610/0009) show a similar arrangement to that in the large specimen, but the jugular canal was probably not completely enclosed in bone.

An isolated small, approximately rectangular and curved bone, is regarded as a basioccipital (NHMW 2013/0609/0007, Text-fig. 6A), and two squarish ossification, the smallest one with a slightly curved margin, are identified as anterior and a posterior catazygals, respectively (NHMW 2013/0609/0008 and NHMW 2013/0609/0009, Text-figs 6B and C).

A reconstruction of the neurocranium is presented in Text-fig. 7.

Suspensorium: A pair of large quadrates, with their associated pterygoids (NHMW 2013/0609/0011 and NHMW 2013/0609/0012, Text-fig. 8), a small right quadrate and pterygoid, and a small left isolated quadrate (NHMW 2013/0610/0002 and NHMW 2013/0610/0003, respectively) are preserved. As usual in coelacanth, the quadrate has a double condyle for articulation with the lower jaw.

The pterygoid (Text-fig. 8) possesses a large overlapping sutural zone with the quadrate. In a specimen with both bones detached, strong ridges cover the overlapping zone for a better attachment between both ossifications. The lateral face of the pterygoid bears a very strong curved ridge. Other coelacanth, such as *Latimeria*, also possess such a strong ridge, which delimits a cartilaginous plate on which several bundles of the ad-

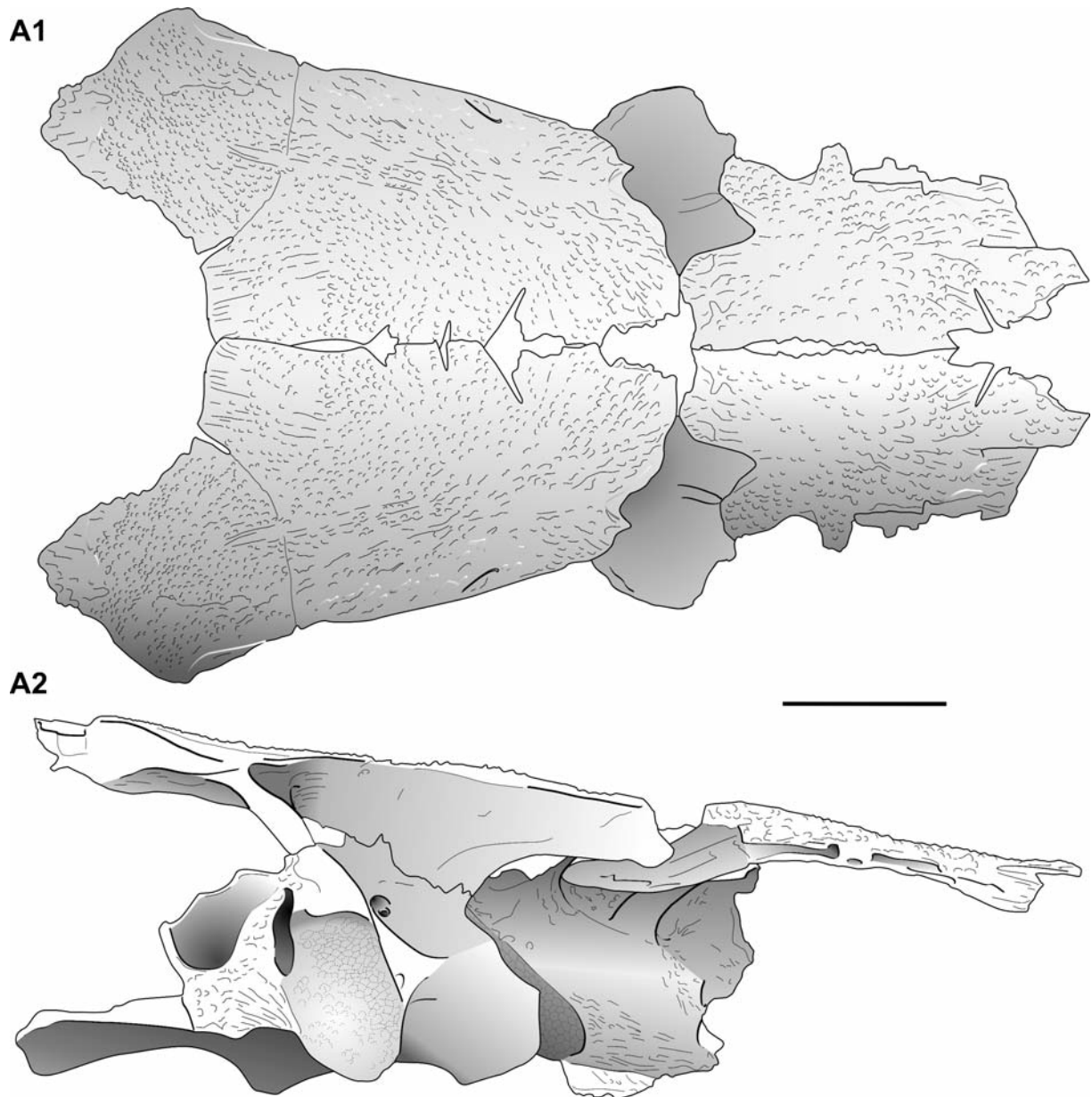
ductor muscle insert (Millot and Anthony 1958; Dutel *et al.* 2013). The medial face of the pterygoid is covered with a shagreen of small teeth, except along a band following the contact with the quadrate. The ventral margin of the pterygoid is gently curved, and no process is present contrary to most latimeriids (Dutel *et al.* 2012).

A pair of triangular bones is regarded as autopalatines (NHMW 2013/0609/0013, Text-fig. 9A). The anterior extremity forms a spine and a crest runs along the medial(?) face.

A dentigerous elongated ossification is identified as a probable right ectopterygoid (NHMW 2013/0609/0014, Text-fig. 9B). The bone bears on its oral face an elongated patch of teeth. A row of proportionally larger teeth, posteriorly inclined, is present along one edge of the patch and along half the length of another edge, but no fangs are present. In between lie numerous small pointed teeth. The aboral face bears a strong ridge defining a groove into which the pterygoid presumably fitted.

The posterior extremity of a parasphenoid (NHMW 2013/0609/0010) perfectly fits the basisphenoid. It is composed of a regularly curved thin sheet of bone with an external (ventral) surface bearing faint ridges and with paired dorsolateral areas with coarse ridges suturing with the basisphenoid. The more anterior portion of the bone is broken.

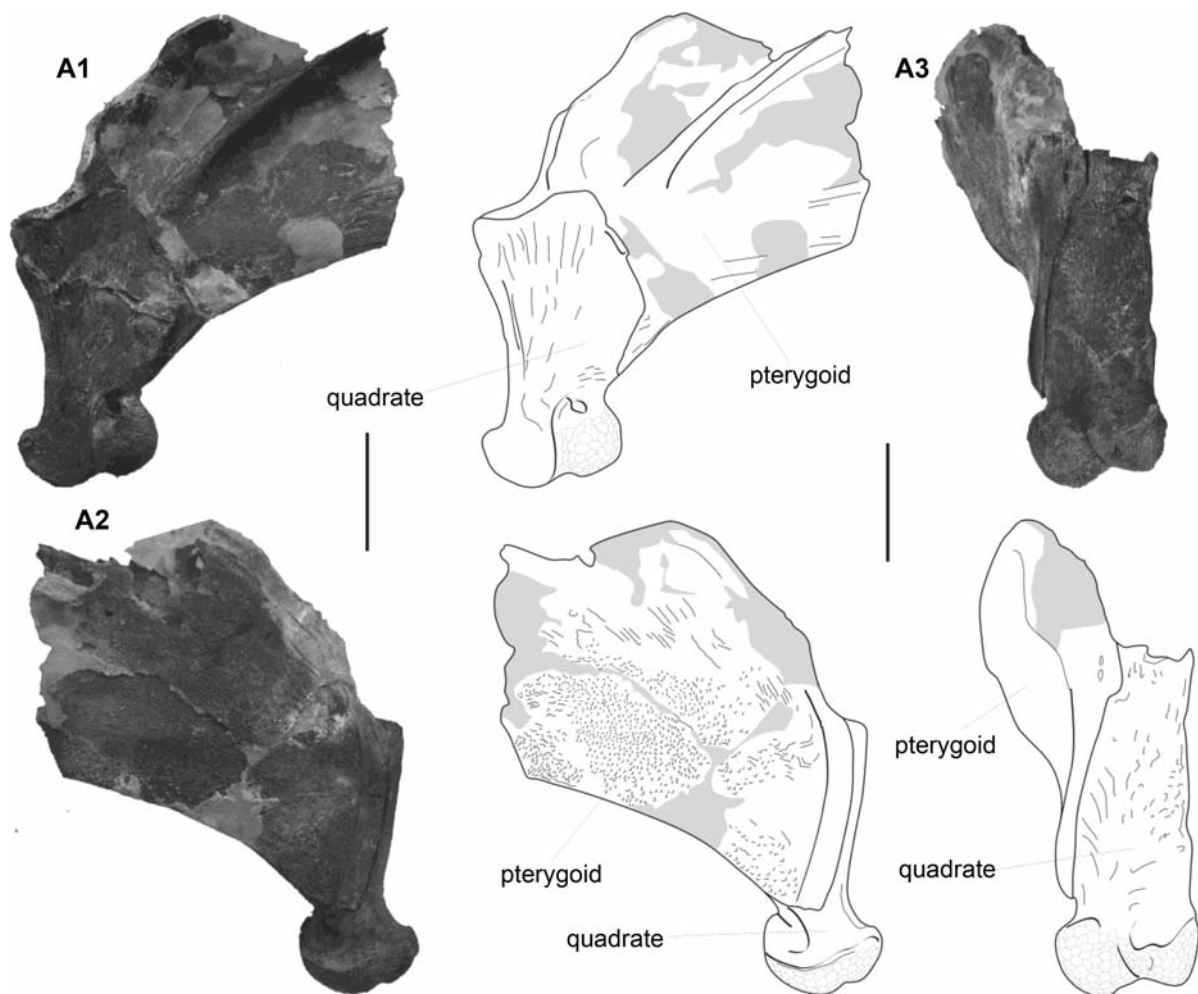
Lower jaw: Both angulars of the large individual (NHMW 2013/0609/0015 and NHMW 2013/0609/0016, Text-fig. 10 A and B), and both of the small one (NHMW



Text-fig. 7. Reconstruction of the skull roof and braincase (without the anterior part) of the actinistian fish *Dobrogeria aegyssensis* gen. et sp. nov. in dorsal (1) and lateral (2) views. The dorsal view has been reconstructed by mirroring the preserved bones. Scale bar: 20 mm

2013/0610/0004 and NHMW 2013/0610/0005, Text-fig. 10C) are preserved. They show different outlines. The angular of the large specimen is shallow with a low coronoid expansion, and the ossification forms an open angle with its ventral margin gently concave in its middle part. On the internal side a ridge runs along the whole length of the bone. It is broader in the posterior half of the ossification. The groove for the external mandibular ramus of the VII nerve is present ventrally to the ridge. Pores in the bottom of the groove accommo-

date lateral branches that supplied the neuromasts of the mandibular sensory canal. The lateral face is ornamented with faint, anastomosed ridges and a few tubercles linearly arranged. A few, five or possibly six, small and elongated foramina for the mandibular sensory canal are visible. The canal, enclosed in the angular, enters in a rather high position on the posterior margin of the bone, then runs along a line parallel to the ventral margin and exits almost in the mid-length of the anterior margin. An oral pit line is not visible in the large specimen



Text-fig. 8. Photographs and semi-interpretative line drawings of the right quadrate and pterygoid of the actinistian fish *Dobrogeria aegyssensis* gen. et sp. nov., NHMW 2013/0609/0011 (holotype) in lateral (A1), medial (A2), and posterior (A3) views; Tulcea Veche Limestone, Lower Spathian, Tulcea. Scale bars: 20 mm

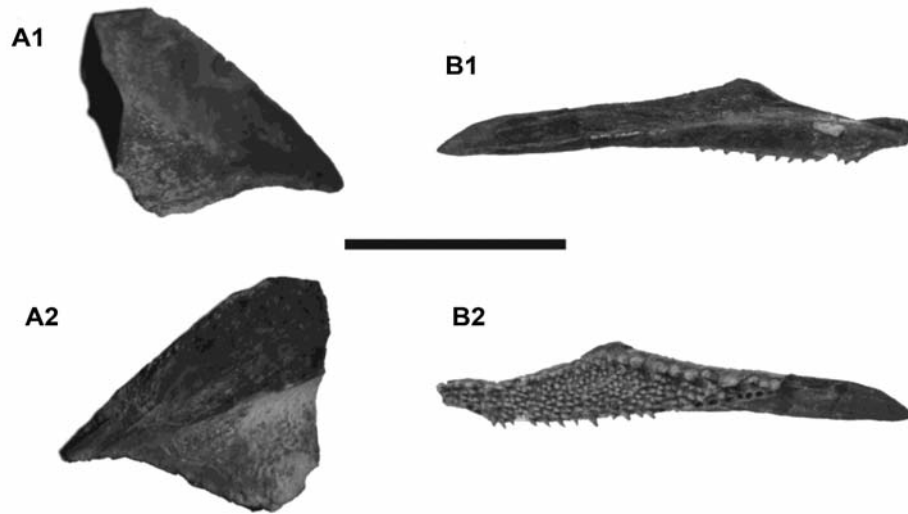
because of the state of preservation of the external surface.

The angulars of the small individual are proportionally deeper, more angled, and with a more developed coronoid expansion than on the large specimen. On the internal side of the bone, the ridge is rounded in section along its posterior portion and sharp in its anterior portion. The external face shows tiny tubercles and faint ridges posteriorly. The mandibular sensory canal enters the bone at the level of the internal ridge, i.e. rather high, then opens via five elongated pores very close to the ventral margin and exits anteriorly at the level of a well-developed ridge at the anterior tip of the bone. An oral pit line is visible in the smaller specimen as a short groove located on the posterior half of the ossification (Text-fig. 10C1).

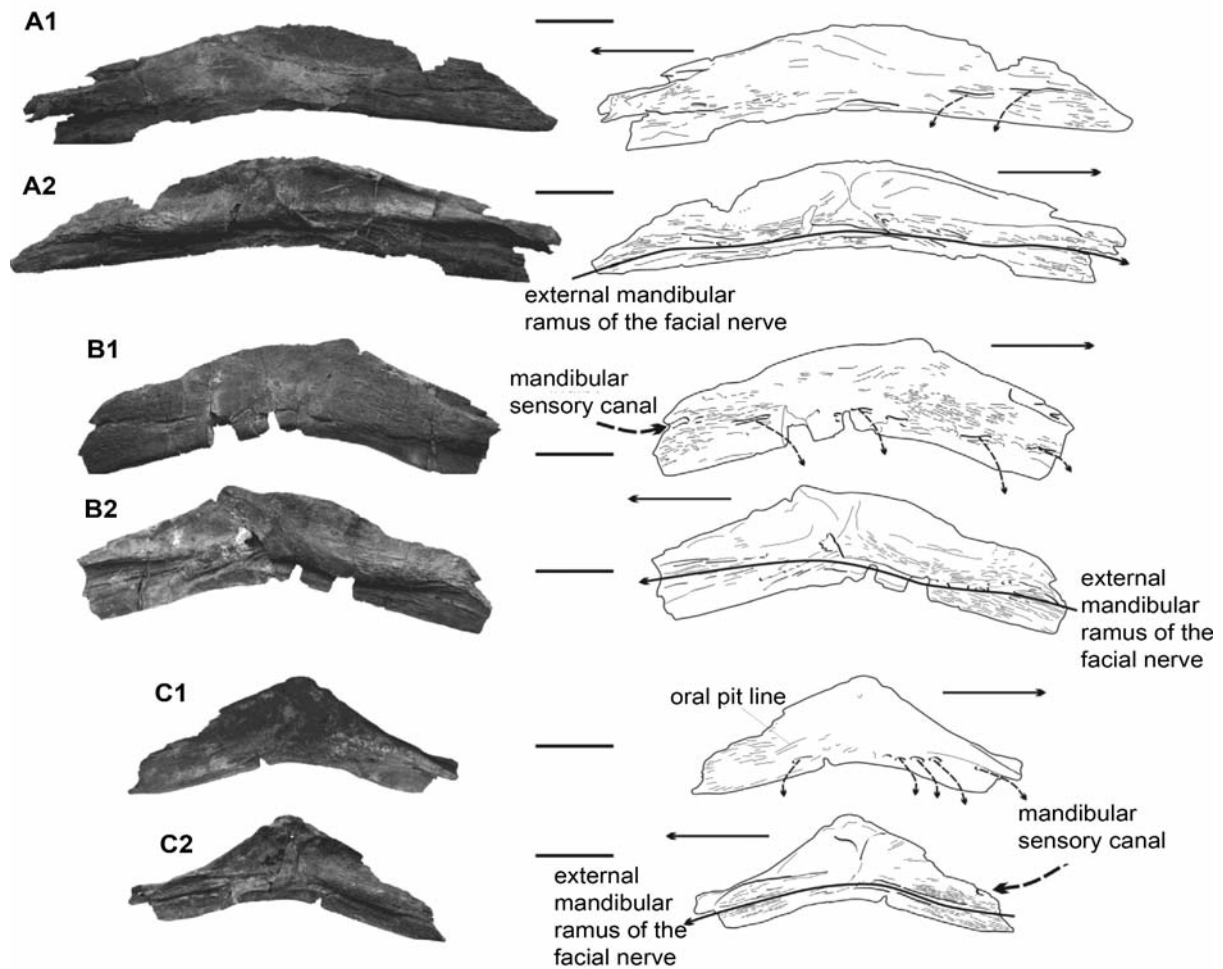
A left splenial fits well in a notch of one of the large angular (NHMW 2013/0609/0017, Text-fig. 11A). The

posterior extremity of the bone tapers to a spine. In the middle of the ossification, both margins are parallel and the bone turns ventrally and inwards and is slightly enlarged at its anterior extremity. The pores of the mandibular sensory canal open along the dorsal margins, and a single pore opens in the middle of the symphysis. A larger pore, situated on the posterior third of the dorsal margin of the ossification and which opened exteriorly between the dentary and the splenial, is the dentary sensory pore. The lateral surface of the angular and splenial are rugose. A club-shaped bone with an articular facet is presumably identified as an articular (NHMW 2013/0609/0018, Text-fig. 11B), although this interpretation remain uncertain.

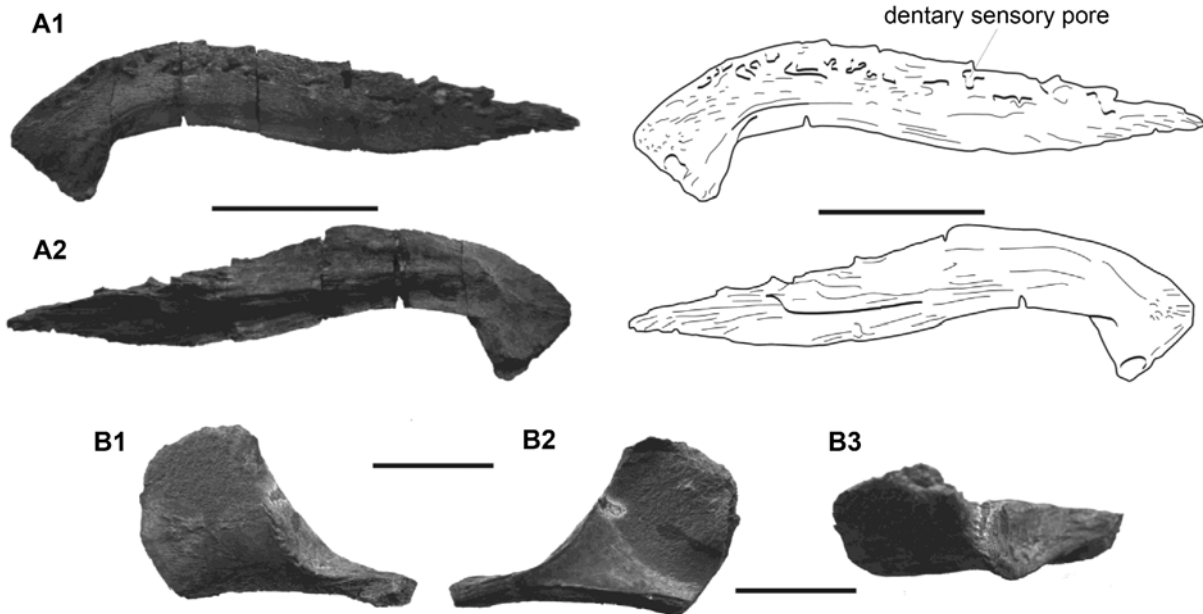
One complete and one incomplete gular, presumably from the same large individual, are preserved (NHMW 2013/0609/0019 and NHMW 2013/0609/0020, Text-fig. 12). They have an approximately triangular outline,



Text-fig. 9. Photographs of the autopalatine (NHMW 2013/0609/0013, A) and right ectopterygoid (NHMW 2013/0609/0014, B) of the actinistian fish *Dobrogeria aegyssensis* gen. et sp. nov. (holotype), unknown views, except B2 in occlusal view; Tulcea Veche Limestone, Lower Spathian, Tulcea. Scale bars: 20 mm



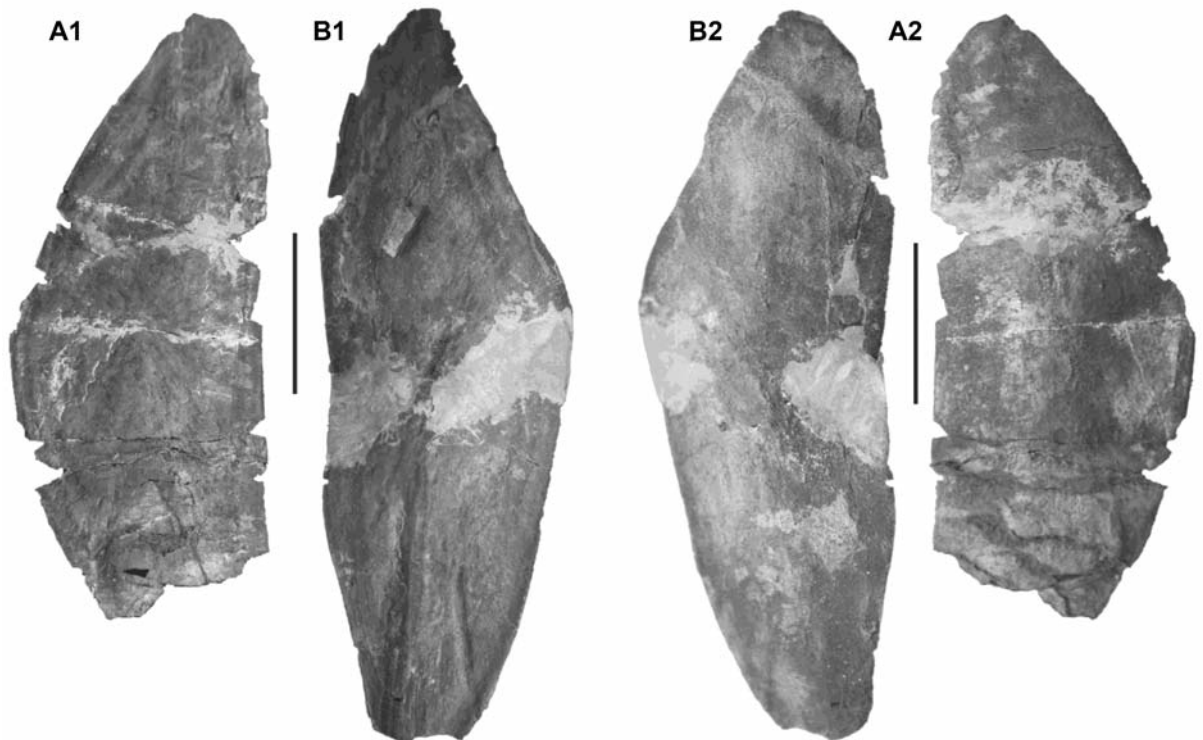
Text-fig. 10. Photographs and semi-interpretative line drawings of the left (A) and right (B and C) angulars at different growth stages of the actinistian fish *Dobrogeria aegyssensis* gen. et sp. nov. (A and B, NHMW 2013/0609/0015 and NHMW 2013/0609/0016 (holotype); C, NHMW 2013/0610/0004) in lateral (1) and medial (2) views; Tulcea Veche Limestone, Lower Spathian, Tulcea. Scale bars: 20 mm



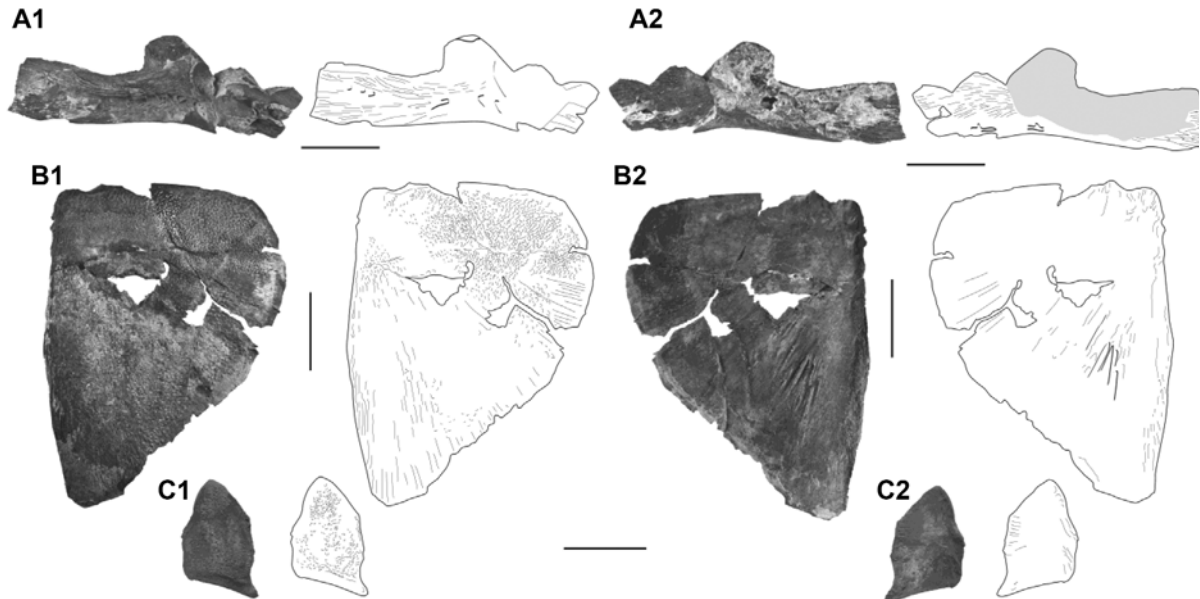
Text-fig. 11. Photographs and semi-interpretative line drawings of left splenial (A) in lateral (1) and medial (2) views, and photographs of the articular (B) in unknown views of the actinistian fish *Dobrogeria aegyssensis* gen. et sp. nov. (holotype: A, NHMW 2013/0609/0017 and B, NHMW 2013/0609/0018); Tulcea Veche Limestone, Lower Spathian, Tulcea. Scale bars: 20 mm

with a regularly rounded anterior margin and a more tapering posterior extremity. They are ca three times longer than wide, making them proportionally wide and com-

parable to *Megalocoelacanthus* from the Turonian of Mexico (Schultze *et al.* 2010; Hauser and Martill 2013). In most other actinistians with preserved gular plates,



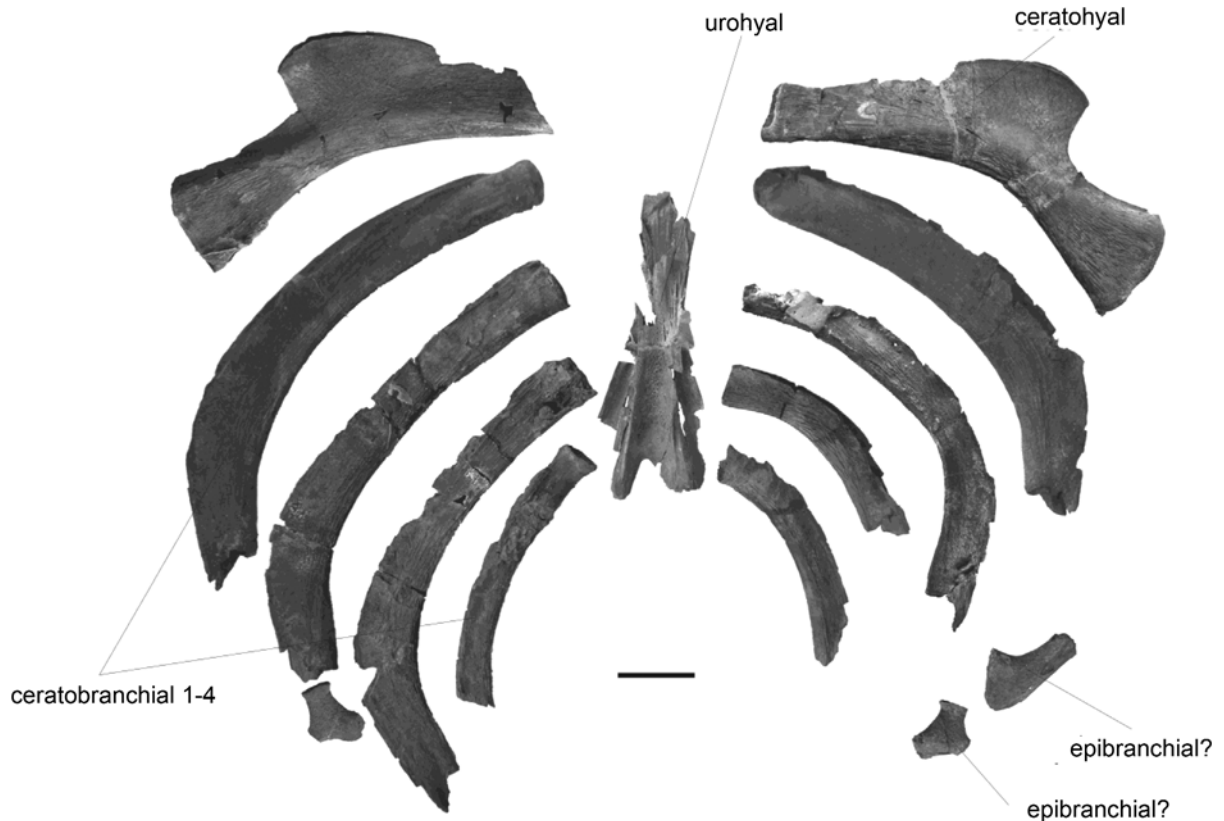
Text-fig. 12. Photographs of right (A) and left (B) gulars of the actinistian fish *Dobrogeria aegyssensis* gen. et sp. nov. (holotype: A, NHMW 2013/0609/0019 and B, NHMW 2013/0609/0020), in internal (dorsal) (1) and ventral (2) views, anterior points to the bottom; Tulcea Veche Limestone, Lower Spathian, Tulcea. Scale bars: 20 mm



Text-fig. 13. Photographs and semi-interpretative line drawings of lachrymojugal (NHMW 2013/0609/0021, A), opercle (NHMW 2013/0609/0022, B) and subopercle (NHMW 2013/0609/0023, C) of the actinistian fish *Dobrogeria aegyssensis* gen. et sp. nov. (holotype) in lateral (1) and medial (2) views; Tulcea Veche Limestone, Lower Spathian, Tulcea. Scale bars: 20 mm

these are proportionally narrower (Hauser and Martill 2013). A ridge runs in across the middle width of the anterior part of the internal side, which is comparable to the

insertion point of the anterior and posterior ramus of the intermandibular muscle observed by Dutel *et al.* (2012) in *Latimeria* and *Megalocoelacanthus*.



Text-fig. 14. Branchial apparatus, NHMW 2013/0609/0024 – NHMW 2013/0609/0028 (holotype); Tulcea Veche Limestone, Lower Spathian, Tulcea. Views variable and uncertain. Scale bar: 20 mm

Cheek and opercular series: A poorly preserved and incomplete ossification is identified as a right lachrymojugal (NHMW 2013/0609/0021, Text-fig. 13A). The extremities are missing and the remaining part is roughly rectangular, with a dorsal rounded process tilted slightly posteriorly. The external face is ornamented with longitudinal grooves, with a large sensory pore posteriorly oriented, as well as several smaller pores more anteriorly. The medial face, strongly damaged, shows preserved areas with an ornamentation forming an elongated reticulated pattern. The anterior portion is expanded and angled.

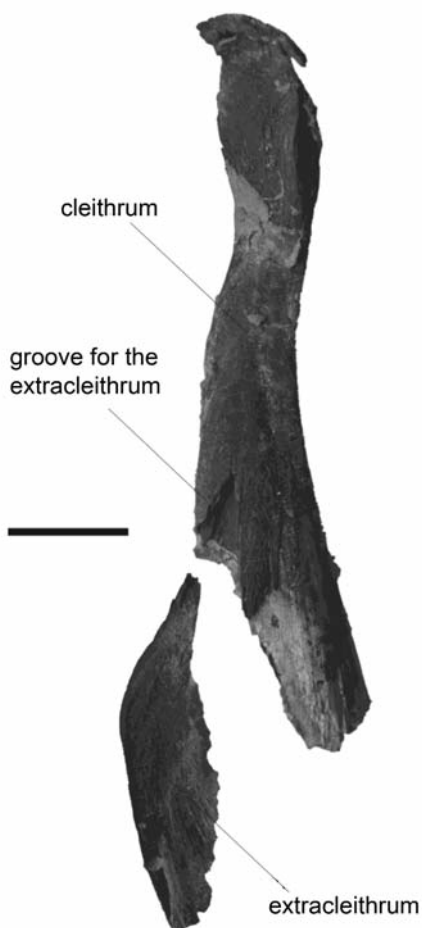
A left opercle (NHMW 2013/0609/0022, Text-fig. 13B) has a right triangle shape, the right angle being formed by the anterodorsal corner. The dorsal and anterior margins are straight, and the posterior margin is slightly rounded in its dorsal portion and straight in its ventral portion. The external surface is ornamented

with dense tubercles in the central and dorsoposterior area, and with faint radiating ridges in its anteroventral area. The shape of the opercle of *Dobrogeria* is reminiscent to the opercle of some Triassic coelacanths, such as *Laugia* and *Coelacanthus*. An irregularly shaped bone is identified as a subopercle because of its general outline, with a tapering extremity, with its external surface ornamented with tubercles and its absence of sensory canal and pit-line (NHMW 2013/0609/0023, Text-fig. 13C).

Other thin plate-like bone fragments belong to the cheek series, but they cannot be precisely identified (postorbital, squamosal, preopercle). They bear a well-developed tubercular ornamentation and the preserved margins indicate that the ossifications were not sutured to each other.

Hyoid and branchial arches: Branchial elements of the large specimen (holotype) are present but not preserved in connection. A restoration of the branchial arches with the preserved bones is presented in Text-fig. 14, keeping in mind that the positions of some of the elements are uncertain and that elements from several individuals can be mixed up, although this latter hypothesis is unlikely. Ceratohyals are stout ossifications, with a long and broad lateral process and an expanded distal extremity. They are reminiscent of the ceratohyal of *Megalocoelacanthus* (Dutel *et al.* 2012). We reconstructed four pairs of broad ceratobranchials (but a fifth pair was probably present), which are excavated by a deep groove for the branchial artery and which are strongly curved in the distal third. A rod-like ossification with an expanded extremity and two others, which are triradiate, are regarded as epibranchial, possibly the first and the second one respectively, but these identifications should be regarded with caution. The urohyal is poorly preserved, but it shows the typical bifid posterior extremity, with a V-shaped slit between both processes. On the dorsal surface, two ridges run from the tip of the posterior processes and slightly converge toward the centre of the bone.

Pectoral girdle: A pair of large cleithra (NHMW 2013/0609/0029, Text-fig. 15), without their ventral extremity, plus fragments of several smaller ones are present. The dorsal extremity is rounded, but not enlarged as in *Ticinepomis* (Cavin *et al.* 2013). The vertical branch is slightly sigmoidal and a triangular groove is dug on the posterior margin, at the level of the enlargement of the bone. The groove accommodated the extracleithrum. A splint-like bone with a rounded margin and two sutural surfaces is an extracleithrum, as confirmed by the shape of one of its extremities, which fits with the groove of the cleithrum (NHMW 2013/0609/0031, Text-fig. 15).



Text-fig. 15. Photographs of right cleithrum (NHMW 2013/0609/0029) and extracleithrum (NHMW 2013/0609/0031–31) of the actinistian fish *Dobrogeria aegysensis* gen. et sp. nov. (holotype) in lateral view; Tulcea Veche Limestone, Lower Spathian, Tulcea. Scale bar: 20 mm

PHYLOGENETIC ANALYSIS

In order to explore the phylogenetic relationships of *Dobrogeria aegyssensis* with other coelacanth, we performed a cladistic analysis. The original datamatrix is from Forey (1998), with modifications from subsequent works (see below). We added the terminal taxa *Swenzia*, *Hoplopterygius*, *Guizhoucoelacanthus*, *Parnaibaia* and *Rebellatrix* (Clément 2005; Friedman and Coates 2006; Liu *et al.* 2006; Yabumoto 2008; Wendruff and Wilson 2012, respectively). We also included *Luopingcoelacanthus* and *Yunnancoelacanthus*, two taxa described by Wen *et al.* (2013). These authors coded the presence of intertemporal bones in *Luopingcoelacanthus*, state 1 for character 12, while the bone located in the supposedly position of an intertemporal in their fig. 3 is described and labelled as a fragment of postorbital. Consequently, we coded this character 0 for *Luopingcoelacanthus*. We added to the original datamatrix the characters 109 (Friedman and Coates 2006) and 110 (Dutel *et al.* 2012), with corrections of coding from Clément (2005) and Brito *et al.* (2010). Additional coding were made by Cavin *et al.* (2013) for *Ticinepomis* and character corrections were proposed by Wendruff (2013) for *Piveteauia* on the basis of previous descriptions. We added character states for *Euporosteus* from Zhu *et al.* (2012).

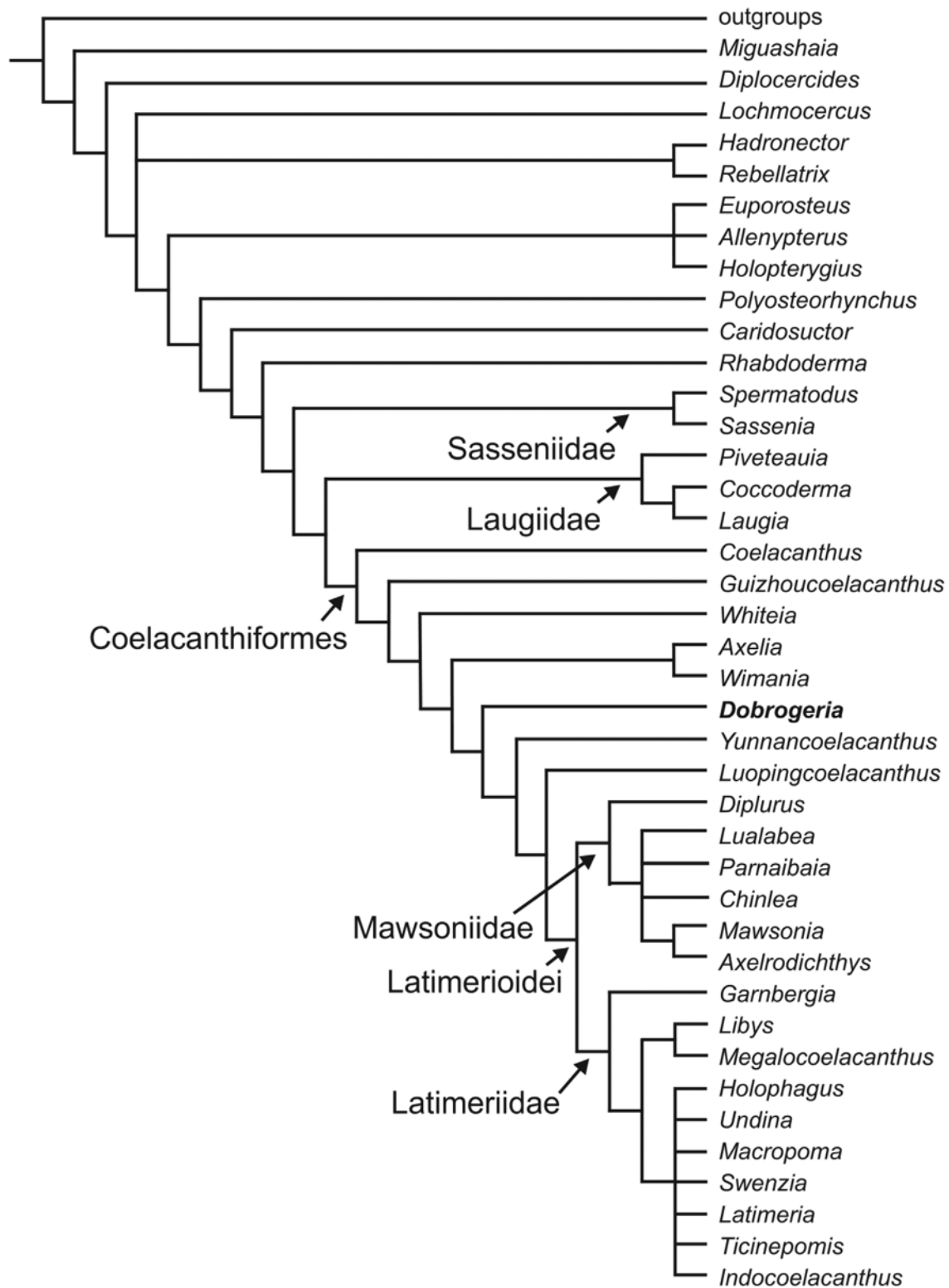
Guizhoucoelacanthus was described by Liu *et al.* (2006) and its characters were coded by Geng *et al.* (2009). We notice that several character codings for *Guizhoucoelacanthus*, also used in Wen *et al.* (2013) and in Cavin *et al.* (2013), were in discrepancy with the description and the figures of Geng *et al.* (2009). Geng *et al.* coded *Guizhoucoelacanthus* as having anterior and posterior parietals of dissimilar size (char. 8) while their description and figures clearly mentioned two pairs of parietals of similar size. They mentioned the occurrence of a quadratojugal (char. 33) while this ossification is not described and figured. We also modified the original coding of character 32, absence or presence of a subopercle, by including a question mark because Geng *et al.* mentioned in the text that this bone is ‘not preserved’, and character 43, position of the postorbital relative to the intracranial joint, because Geng *et al.*’s figure 2 clearly shows that the postorbital spans the joint. We coded character 44, ‘infraorbital canal in the postorbital with simple pore opening directly from the main canal’ (coded with a ‘?’ in Geng *et al.*), because this character state is described in the text.

Eventually, we reversed the definition by Forey of the states of character 71 (‘processus connectens meeting parasphenoid (0), failing to meet parasphenoid

(1)’) because we noticed that the coding for the taxa were opposite to the definition. The resulting character list is presented in Appendix 2.

The outgroups are those used by Forey (1998), i.e. *Mimia* (Actinopterygii) and Porolepiformes. No details are provided by Forey about the taxa used for coding the porolepiform characters. This coding may not represent one single taxon, but character states observed on several taxa. Ideally, terminal taxa should be species, but they may represent supra-specific taxa (genera for most of the terminal ingroup taxa compared here), when taxic or methodological issues occur (Forey 1998, p. 230). The resulting datamatrix is presented in Appendix 3.

The strict consensus tree of the 1668 most parsimonious trees (311 steps, CI=0.3826, RI=0.6784) is on the whole weakly supported, with Bremer decay indices of 1 for all the nodes (Text-fig. 16). It shows a pattern mostly in accordance with recent phylogenetic studies of Actinistia. The phylogenetic position of *Dobrogeria* is as follows: *Dobrogeria* (*Yunnancoelacanthus* (*Luopingcoelacanthus* Latimerioidei)), with the Latimerioidei defined as the least inclusive clade containing *Latimeria chalumnae* and *Mawsonia gigas* (Dutel *et al.* 2012). *Dobrogeria* and more derived actinistians share two unambiguous characters, – ‘presence of a postparietal descending process’ (char. 13, ci = 0.5) and ‘an anteriorly expanded lachrymojugal’ (char. 35, ci = 0.5), plus two ambiguous characters (char. 23 and 104). *Yunnancoelacanthus* and more derived actinistians share a single unambiguous character – ‘absence of a suboperculum’ (char. 32, ci = 0.250) – and one ambiguous character (char. 59). *Luopingcoelacanthus* and more derived actinistians share two unambiguous characters, – ‘anterior and posterior pairs of parietals similar in size’ (char. 8, ci = 0.167) and ‘hooked-shape dentary’ (char. 57, ci = 0.333), plus two ambiguous characters (char. 10 and 51). The clade Latimeriidae has the same content as in Dutel *et al.* (2012) and Cavin *et al.* (2013), except that in the former study *Garnbergia* is located as the sister group of latimerioids, while it is located as the sister-group of all other latimeriids here. *Libys* and *Megalocoelacanthus* form a clade supported by the same unambiguous (char. 23, 50, 68) and ambiguous (char. 2, 39, 49, 68, 70 and 89) characters as those found by Dutel *et al.* (2012), plus the ambiguous character 99. Other Latimeriid genera, including here *Indocoelacanthus*, are placed in a polytomy. The node corresponding to the Latimeriidae is supported by same ambiguous characters (char. 3, 22, 30, 60 and 110) as those found by Dutel *et al.* (2012). Differences with the latter analysis is that characters 79 and 103 do not support this



Text-fig. 16. Phylogenetic analysis based on 42 taxa and 110 characters. Strict consensus tree of the 1668 shortest trees (length 312; consistency index = 0.3826; retention index of 0.6784; Bremer decay indices for all nodes equal 1). Some major clade names are indicated

node in our study, while character 104 – ‘scale ornament not differentiated’ – does support it. Characters 60 – ‘presence of a subopercular branch of the mandibular sensory canal’ – and 110 – ‘ventral swelling of the palatoquadrate’ are found exclusively within the latimeriids ($ci = 1$). The content and relationships of the Mawsoniidae, including here the genus *Lualabea*, are similar to those found by Dutel *et al.* (2012), Wen *et al.* (2013) and Cavin *et al.* (2013). The node corresponding to this family is supported by the same unambiguous characters as those found by Dutel *et al.* (2012) (Char. 14, 56, 92), but in our study character 104 does not support the node, while character 79 supports it.

The basalmost part of the cladogram, dealing with the Palaeozoic taxa, is on the whole similar to the pattern obtained in recent studies, in particular by Dutel *et al.* (2012) and by Cavin *et al.* (2013). Most of the genera are placed at successive nodes, with *Miguashaia* as the sister-group of all other actinistians. We found here *Hadronector* and *Rebellatrix* forming a clade resolved in a trichotomy with *Lochmocercus* and the more derived Actinistia. A single unambiguous character support the sister-pair *Hadronector* and *Rebellatrix*, - ‘an anteriorly forked basal support for D2’ (char. 102, $ci = 0.5$) - and two ambiguous characters (char. 23 and 91). Another difference between the Dutel *et al.* (2012) and Cavin *et al.* (2013) studies and the present one is that here *Diplocercoides* is not the sister genus of *Euporosteus*, but *Euporosteus* is placed in a trichotomy with *Holopterygius* and *Allenpyterus*. This node is supported by two unambiguous characters – ‘middle and posterior pit lines within posterior half of postparietals’ (char. 25, $ci = 0.29$) and ‘ventral keel scales’ (char. 109, $ci = 1$) –, as well as by eight ambiguous characters (char. 8, 29, 42, 48, 49, 50, 58 and 94). *Polysteorhynchus*, *Caridosuctor* and *Rhabdoderma* are placed at successive nodes in the present study, as in both papers quoted above. *Rhabdoderma* is the sister taxon of all post-Palaeozoic taxa, a pattern also found in most recent studies (Forey 1998; Schultze 2004; Clément 2005; Yabumoto 2008; Geng *et al.* 2009; Dutel *et al.* 2012; Wen *et al.* 2013; Cavin *et al.* 2013). *Rhabdoderma* and post-Palaeozoic taxa form a node supported by one unambiguous character, a ‘splenial without ornament’ (char. 64, $ci = 0.333$). The next node, which groups Sasseniidae (*Spermatodus* and *Sassenia*) and more derived taxa is supported by a unique unambiguous synapomorphy – ‘the angular with granular ornaments’ (char. 62, $ci = 1$) – and by one unambiguous character with a single parallel evolution in the clade defined above (*Holopterygius*, *Euporosteus*, *Allenpyterus*) – ‘cheek

bones separated from one another’ (char. 29; $ci = 0.5$). Three ambiguous characters (char. 18, 101 and 105) also support this node. The next node groups Laugiidae and the more derived Actinistia. The Laugiidae comprises here three genera arranged as follows: *Piveteauia* (*Laugia Coccooderma*). This family is supported by 4 unambiguous characters (char. 45, 48, 91, 100), one – ‘pelvic fins abdominal’ (char. 100, $ci = 1$) – being unique among actinistia (Forey 1998). Three ambiguous characters also support this node (char. 32, 96 and 108), one – ‘pelvic bones of each side fused in midline’ (char. 108, $ci = 1$) – being also unique for this node. The next node groups *Coelacanthus* with the more derived Actinistia. It is supported by two unambiguous characters (char. 1 and 21), and 8 unambiguous ones (char. 27, 70, 71, 76, 77, 78, 82 and 86), three of them (char. 71, 82 and 86) being unique for this clade ($ci = 1$).

Coelacanthus, *Guizhoucoelacanthus* and *Whiteia* are placed at successive nodes in the consensus tree. The node supporting *Guizhoucoelacanthus* and more derived Actinistia is supported by 4 unambiguous (char. 8, 36, 96 and 97) and 1 ambiguous (char. 53) characters, and the node supporting *Whiteia* and more derived Actinistia is supported by 2 unambiguous (char. 15 and 98) and two ambiguous (char. 27 and 59) characters. In some previous studies, these genera show a similar phylogenetic pattern to the pattern found here (Forey 1998; Clément 2005; Yabumoto 2008 in one of his analysis, with *Guizhoucoelacanthus* absent in the three studies; Wen *et al.* 2013). In Geng *et al.* (2009) and Dutel *et al.* (2012), *Piveteauia*, *Whiteia* and *Guizhoucoelacanthus* are grouped together in a clade named ‘Whiteiidae’ by Geng *et al.* (2009) (*Axelia* and *Wimania* are also included in this clade in Dutel *et al.*’s analysis). In our analysis, *Axelia* and *Wimania* form a clade as in Schultze (2004), but in the latter study the clade also contains *Coelacanthus* and *Ticinepomis* (the ‘Coelacanthidae’ according to this author), which are located elsewhere here. The sister-group relationships of *Axelia* and *Wimania* is supported here by 1 unambiguous (char. 7, $ci = 0.333$) and 1 ambiguous (char. 31, $ci = 0.333$) characters. The node formed by the clade (*Axelia Wimania*) and more derived Actinistia is supported by a single unambiguous character – ‘more than seven extrascapulars’ (char. 17, $ci = 0.4$) – and four ambiguous characters (char. 26, 48, 79 and 96). More derived Actinistia are resolved as follows: *Dobrogeria* (*Yunnancoelacanthus* (*Luopingcoelacanthus* Latimerioidei)). In Wen *et al.* (2013) and Cavin *et al.* (2013), the relationships were as follows: (*Luopingcoelacanthus* (*Yunnancoelacanthus* Latimerioidei)).

DISCUSSION

Other Triassic coelacanths regarded as valid taxa by Forey (1998), but not included in the phylogenetic analysis conducted here, can be compared with *Dobrogeria*. *Moenkopia wellesi* was described by Schaeffer and Gregory (1961) on the basis of isolated bones, in particular basisphenoids, from the Early Anisian Moenkopi Formation in Arizona, USA. The basisphenoid of *Moenkopia* differs from that of *Dobrogeria* by a long dorsum sellae plus corpus distance, a narrow pituitary notch between the antotic processes, a nearly rectangular antotic processes in dorsal view (proportionally larger and rounder in *Dobrogeria*). Both genera share rounded and prominent sphenoid condyles. *Osteopleurus*, from the Upper Triassic of the Newark Group, USA (Schaeffer 1941; Shainin 1943), regarded as a synonym of *Diplurus* by Forey (1998), and *Alcoveria*, from the Spanish Muschelkalk (Forey 1998), are incompletely preserved taxa, which can be differentiated from *Dobrogeria* by the shape of their opercles, among other characters. *Graphiurichthys*, from the Late Triassic of Raibl, Austria, can be separated by the skull bones ornamented with narrow tubercles. *Mylacanthus* and *Sceleracanthus*, from the Early Triassic of Spitzbergen, are closely related, or synonymous, to *Axelia* (Forey 1998), a genus which is located in a more basal position in our phylogeny. *Hainbergia* and *Heptanema*, from the Middle Triassic of Germany and Italy, respectively, *Sinocoelacanthus* from the Early Triassic of Guangxi, China, are too incompletely preserved to be compared with *Dobrogeria*.

On the basis of the phylogenetic analysis and on comparisons with other taxa based on less complete material, the taxon described here can confidently be referred to a new genus and new species. However, it cannot be assigned to a family because this part of the cladogram shows genera at successive nodes in the consensus tree and show different patterns according to analyses (Dutel *et al.* 2012; Wen *et al.* 2013; Cavin *et al.* 2013; present study).

In our analysis, the Laugiidae contain the same three genera as those considered by Forey, i.e. *Piveteauia* (*Coccoderma*, *Laugia*). Recently *Belemnocerca prolata* was included in this family by Wendruff and Wilson (2013), but has not been included in our cladistic analysis. Schultze (2004) included the laugiids within the coelacanthiforms, but we prefer here to retain the clade Coelacanthiformes as defined by Forey, i.e. not containing the laugiids, because it is based on a relatively well-supported node. In particular, we found in our analysis the neurocranial charac-

ters used by Forey in his diagnosis of coelacanthiforms, such as ‘supraoccipital present’ (char. 76, ci = 1), ‘vestibular fontanelle absent’ (char. 77, ci = 0.5), ‘buccohypophysial canal closed’ (char. 78, ci = 0.5), ‘prootic with a complex suture with the basioccipital’ (char. 82, ci=1), and ‘separate basioccipital’ (char. 86, ci = 1).

Rebellatrix divaricerca is an unusual fork-tailed coelacanth from the Lower Triassic of Canada known mostly by post-cranial characters (Wendruff and Wilson 2012). A cladistic analysis by Wendruff and Wilson (2012) resolved *Rebellatrix* as the sister-group of Latimerioidei on the basis of a single shared character, ‘expanded occipital neural arches’ (char. 91). In our analysis, the position of *Rebellatrix* is very different, i.e. placed as the sister-genus of the Carboniferous *Hadronector* (see above for details). Although this position is weakly supported, it suggests an interesting concurrent hypothesis, i.e. that *Rebellatrix* is a representative of an old and basal lineage of Actinistia. More material of *Rebellatrix*, including cranial remains, are necessary for testing both hypotheses.

CONCLUSION

The actinistian material described here is well preserved, but difficult to compare with most other coelacanth taxa which are, for the most part, preserved as articulated specimens. However, the new material possesses characters that support the assignment of these specimens to a new species and new genus, *Dobrogeria aegyssensis*. This new coelacanth increases the taxic diversity of the group in the Early Triassic, which is the time interval with the highest peak of diversity. The inclusion of *Dobrogeria* in a phylogenetic analysis of the actinistians indicates that it is a non-latimerioid coelacanthiform. The cladistic analysis recovered clades which are found in most recent analyses, i.e. the Sasseniidae, the Laugiidae, the Coelacanthiformes, the Latimerioidei, the Mawsoniidae and the Latimeriidae. The regions of the cladogram showing most variation with respect to previous studies are basal coelacanthiforms (*Coelacanthus*, *Guizhoucoelacanthus*, *Whiteia*, *Axelia*, *Wimania*, *Dobrogeria*, *Yunnancoelacanthus*, *Luopingcoelacanthus*) and intrarelationships among the latimeriids. *Rebellatrix*, from the Early Triassic of Canada, is resolved here as the sister-genus of the Carboniferous genus *Hadronector*, raising the possibility that this genus is a representative of an old basal lineage of Actinistia.

Acknowledgments

We sincerely thank Hugo Dutel (Kobe) and Andrew Wendruff (Edmonton) for constructive discussion about actinistian morphology and phylogeny, and our reviewers, Zehra Johanson (London) and Hugo Dutel for helpful suggestions and critiques. The second author acknowledges the financial support from the Romanian Academy by the Scientific Grant 368/2001-2002.

REFERENCES

- Brito, P.M., Meunier, F., Clément, G. and Geffard-Kuriyama, D. 2010. The histological structure of the calcified lung of the fossil coelacanth *Axelrodichthys araripensis* (Actinistia: Mawsoniidae). *Palaeontology*, **53**, 1281–1290.
- Cavin, L. and Forey, P.L. 2004. New mawsoniid coelacanth (Sarcopterygii: Actinistia) remains from the Cretaceous of the Kem Kem beds, SE Morocco. In: A. Tintori and G. Arratia (Eds), *Mesozoic fishes 3 – systematics, paleoenvironments and biodiversity*, 493–506. Dr Pfeil Verlag.
- Cavin, L., Furrer, H. and Obrist, C. 2013. New coelacanth material from the Middle Triassic of eastern Switzerland and comments on the taxic diversity of actinistians. *Swiss Journal of Geosciences*, **106**, 161–177.
- Clément, G. 2005. A new coelacanth (Actinistia, Sarcopterygii) from the Jurassic of France, and the question of the closest relative fossil to *Latimeria*. *Journal of Vertebrate Paleontology*, **25**, 481–491.
- Cloutier, R. 1991. Patterns, trends, and rates of evolution within the Actinistia. *Environmental biology of Fishes*, **32**, 23–58.
- Dutel, H., Maisey, J.G., Schwimmer, D.R., Janvier, P., Herbin, M. and Clément, G. 2012. The Giant Cretaceous Coelacanth (Actinistia, Sarcopterygii) *Megalocoelacanthus dobiei* Schwimmer, Stewart & Williams, 1994, and its Bearing on Latimerioidei Interrelationships. *PLoS ONE* **7** (11), e49911.
- Dutel, H., Herrel, A., Clément, G. and Herbin, M. 2013. A reevaluation of the anatomy of the jaw-closing system in the extant coelacanth *Latimeria chalumnae*. *Naturwissenschaften*, **100**, 1007–1022.
- Forey, P.L. 1998. *History of the Coelacanth Fishes*, 419 pp., Chapman and Hall, London.
- Forey, P.L., Monod, O. and Patterson, C. 1985. Fishes from the Akkuyu Formation (Tithonian), Western Taurus, Turkey. *Geobios*, **18**, 195–201.
- Friedman, M. and Coates, M.I. 2006. A newly recognized fossil coelacanth highlights the early morphological diversification of the clade. *Proceedings of the Royal Society, Series B*, **273**, 245–250.
- Grădinaru, E. 1995. Mesozoic rocks in North Dobrogea: an overview. In: M. Săndulescu and E. Grădinaru (Eds), IGCP Project No. 369, *Comparative Evolution of PeriTethyan Rift Basins. Central and North Dobrogea, Romania, October 1–4, 1995. Field Guidebook*, p. 1–4. Bucharest.
- Grădinaru, E. 2000. Introduction to the Triassic Geology of North Dobrogea Orogene. In: E. Grădinaru (Ed.), *Workshop on the Lower-Middle Triassic (Olenekian-Anisian) boundary, 7–10 June 2000, Tulcea, Romania, Conference and Field Trip. Field Trip Guide*, 5–37. Bucharest.
- Grădinaru, E. 2006. *Geologia terenurilor triasice și jurasice din Zona Peceneaga-Camena*. 212 p., Ars Docendi, București.
- Geng, B.-H. and Zhu, M.J. F. 2009. A revision and phylogenetic analysis of *Guizhoucoelacanthus* (Sarcopterygii, Actinistia) from the Triassic of China. *Vertebrata Palasiatica*, **47**, 311–329.
- Hauser, L.M. and Martill, D.M. 2013. Evidence for coelacanths in the Late Triassic (Rhaetian) of England. *Proceedings of the Geologists' Association*, **124**, 982–987.
- Johanson, Z., Long, J., Talent, J., Janvier, P. and Warren, J. 2006. Oldest coelacanth, from the Early Devonian of Australia. *Biology Letters*, **2**, 443–446.
- Kittl, E. 1908. Beiträge zur Kenntnis der Triasbildungen der nordöstlichen Dobrudscha. *Denkschriften der kaiserlichen Akademie der Wissenschaften, mathematisch-naturwissenschaftlichen Klasse*, **81**, 447–532.
- Liu, G.B., Yin, G.Z., Luo, Y.M., Wang, X.H. and Wang, S.Y. 2006. Preliminary examination of fish fossils from Upper Triassic Wayao Member of Falang Formation in Guanling of Guizhou. *Acta Palaeontologica Sinica*, **45**, 1–20. [In Chinese with English summary]
- Maddison, D.R. 1991. The discovery and importance of multiple islands of most-parsimonious trees. *Systematic Zoology*, **40**, 315–328.
- Millot, J. and Anthony, J. 1958. Anatomie de *Latimeria chalumnae*. I. Squelette et muscles. Centre National de la Recherche Scientifique, 122 p. Paris.
- Mirăuță, O. 1966. Dévonien et Trias des collines de Mahmudia (Dobrogea septentrionale). Dări de Seamă ale Ședințelor, Inst. Geol. Rom., **52**, 115–134.
- Reis, O.M. 1900. *Coelacanthus lunzensis* Teller. *Jahrbuch des Kaiserlich-Königlichen Geologischen Reichsanstalt, Wien*, **50**, 187–192.
- Săndulescu, M. 1995. Dobrogea within the Carpathian Foreland. In: M. Săndulescu and E. Grădinaru (Eds), IGCP Project No. 369, *Comparative Evolution of PeriTethyan Rift Basins. Central and North Dobrogea, Romania, October 1–4, 1995. Field Guidebook*, pp. 1–4. Bucharest.
- Schaeffer, B. 1941. A revision of *Coelacanthus newarki* and notes on the evolution of the girdles and basal plates of the median fins in the Coelacanthini. *American Museum Novitates*, **1110**, 1–17.
- Schaeffer, B. and Gregory, J.T. 1961. Coelacanth Fishes from the Continental Triassic of the Western United States.

- American Museum Novitates*, **2036**, 1–17.
- Schaumberg, G. 1978. Neubeschreibung von *Coelacanthus granulatus* Agassiz (Actinistia, Pisces) aus dem Kupferschiefer von Richelsdorf (Perm, W.-Deutschland). *Palaeontologische Zeitschrift*, **52**, 169–197.
- Schultze, H.-P. 2004. Mesozoic sarcopterygians. In: G. Arratia and A. Tintori (Eds), Mesozoic fishes 3 - systematics, paleoenvironments and biodiversity, 463–492. Verlag Dr Friedrich Pfeil, München.
- Schultze, H.-P., Fuchs, D., Giersch, S., Ifrim, C. and Stinnesbeck, W. 2010. *Palaeoctopus pelagicus* from the Turonian of Mexico reinterpreted as a coelacanth (Sarcopterygian) gular plate. *Palaeontology*, **53**, 689–694.
- Şengör, A.M.C. 1984. The Cimmeride Orogenic System and the Tectonics of Eurasia. *Geological Society of America, Special Paper*, **195**, IX + 82 pp.
- Shainin, V.E. 1943. New coelacanth fishes from the Triassic of New Jersey. *Journal of Palaeontology*, **17**, 271–275.
- Simionescu, I. 1908. Über das Vorkommen der Werfener Schichten in Dobrogea (Rumänien). *Verhandlungen der k. k. geolog. Reichsanstalt*, 1908, **7**, 159–161.
- Simionescu, I. 1911. Studii geologice și paleontologice din Dobrogea. V. Fauna triasică inferioară din Dobrogea (La faune du Trias inférieur de Dobrogea). *Academia Română, Publicațiunile Fondului Vasile Adamachi*, **5** (29) (1910–1913), 63–79.
- Simionescu, I. 1913a. Ichthyosaurierreste aus der Trias von Dobrogea (Rumänien). *Bulletin de la Section Scientifique de l'Académie Roumaine*, **1** (2) (1912–1913), 81–86.
- Simionescu, I. 1913b. Studii geologice și paleontologice din Dobrogea. VI. Les ammonites triasiques de Hagighiol (Dobrogea). *Academia Română, Publicațiunile Fondului Vasile Adamachi*, **5** (34) (1910–1913), 271–370.
- Swofford, D.L. 2001. PAUP*: phylogenetic analysis using parsimony and other methods (software). Sinauer Associates, Sunderland.
- Wen, W., Zhang, Q.-Y., Hu, S.-X., Benton, M.J., Zhou, C.-Y., Tao, X., Huang, J.-Y. and Chen, Z.-Q. 2013. Coelacanths from the Middle Triassic Luoping Biota, Yunnan, South China, with the earliest evidence of ovoviviparity. *Acta Palaeontologica Polonica*, **58** (1), 175–193.
- Wendruff, A. 2013. *Lower Triassic Coelacanths of the Sulphur Mountain Formation (Wapiti Lake) in British Columbia, Canada*. Master Thesis, University of Alberta. <http://hdl.handle.net/10048/2033>
- Wendruff, A.J. and Wilson, M.V.H. 2012. A fork-tailed coelacanth, *Rebellatrix divaricerca*, gen. et sp. nov. (Actinistia, Rebellatricidae, fam. nov.), from the Lower Triassic of Western Canada. *Journal of Vertebrate Paleontology*, **32**, 499–511. doi:10.1080/02724634.2012.657317.
- Wendruff, A. J. and Wilson, M. V. H. 2013. New Early Triassic coelacanth in the family Laugiidae (Sarcopterygii: Actinistia) from the Sulphur Mountain Formation near Wapiti Lake, British Columbia, Canada. *Canadian Journal of Earth Sciences*, **50**, 904–910.
- Yabumoto, Y. 2008. A New Mesozoic coelacanth from Brazil (Sarcopterygii, Actinistia). *Paleontological Research*, **12**, 329–343.
- Zhu, M., Yu, X., Lu, J., Qiao, T., Zhao, W. and Jia, L. 2012. Earliest known coelacanth skull extends the range of anatomically modern coelacanths to the Early Devonian. *Nature Communications* **772**. doi: 10.1038/ncomms1764.

Manuscript submitted: 30th November 2013

Revised version accepted: 15th April 2014

Appendix 1

List of ossifications referable to the holotype (NHMW 2013/0609) and to the smaller specimen (NHMW 2013/0610) housed in the Naturhistorisches Museum Wien, Austria.

Holotype, NHMW 2013/0609 (Big individual)

NHMW 2013/0609/0001 – right posterior parietal (1 item)
 NHMW 2013/0609/0002 – left posterior parietal and supratemporal (1 item)
 NHMW 2013/0609/0003 – right posterior parietal and supratemporal (1 item)
 NHMW 2013/0609/0004 – basisphenoid (1 item)
 NHMW 2013/0609/0005 – right prootic (1 item)
 NHMW 2013/0609/0006 – left prootic (1 item)
 NHMW 2013/0609/0007 – basioccipital (1 item)
 NHMW 2013/0609/0008 – anterior anazygal (1 item)
 NHMW 2013/0609/0009 – posterior anazygal (1 item)
 NHMW 2013/0609/0010 – fragment of parasphenoid (1 item)
 NHMW 2013/0609/0011 – right quadrate and pterygoid (1 item)
 NHMW 2013/0609/0012 – left quadrate (1 item)
 NHMW 2013/0609/0013 – autopalatine (1 item)
 NHMW 2013/0609/0014 – left ectopterygoid (1 item)
 NHMW 2013/0609/0015 – left angular (1 item)
 NHMW 2013/0609/0016 – right angular (1 item)
 NHMW 2013/0609/0017 – left splenial (1 item)
 NHMW 2013/0609/0018 – articular (1 item)
 NHMW 2013/0609/0019 – right gular (1 item)
 NHMW 2013/0609/0020 – left gular (1 item)
 NHMW 2013/0609/0021 – lachrymojugal (1 item)
 NHMW 2013/0609/0022 – opercle (1 item)
 NHMW 2013/0609/0023 – subopercle (1 item)
 NHMW 2013/0609/0024 – right ceratohyal (1 item)
 NHMW 2013/0609/0025 – left ceratohyal (1 item)
 NHMW 2013/0609/0026 – ceratobranchial (8 items)
 NHMW 2013/0609/0027 – epibranchial ? (4 items)
 NHMW 2013/0609/0028 – urohyal (1 item)
 NHMW 2013/0609/0029 – right cleithrum (1 item)
 NHMW 2013/0609/0030 – left cleithrum (1 item)
 NHMW 2013/0609/0031 – extracleithrum (1 item)
 NHMW 2013/0609/0032 – right metapterygoid ? (1 item)
 NHMW 2013/0609/0033 – indeterminate ossification of braincase (2 items)
 NHMW 2013/0609/0034 – indeterminate different ossifications (9 items)
 NHMW 2013/0609/0035 – ribs, vertebrate elements and ray fragments

NHMW 2013/0610 (Small individual)

NHMW 2013/0610/0001 – right posterior parietal (1 item)
 NHMW 2013/0610/0002 – right quadrate and pterygoid (1 item)
 NHMW 2013/0610/0003 – left quadrate (1 item)
 NHMW 2013/0610/0004 – right angular (1 item)
 NHMW 2013/0610/0005 – left angular (1 item)
 NHMW 2013/0610/0006 – left supratemporal (1 item)
 NHMW 2013/0610/0007 – left postparietal (pars) (1 item)
 NHMW 2013/0610/0008 – right prootic (1 item)
 NHMW 2013/0610/0009 – left prootic (1 item)
 NHMW 2013/0610/0010 – right articular (1 item)
 NHMW 2013/0610/0011 – left articular (1 item)
 NHMW 2013/0610/0012 – cleithrum (1 item)
 NHMW 2013/0610/0013 – ceratobranchial (1 item)
 NHMW 2013/0619/0014 – indeterminate different ossifications (10 items)

Appendix 2

List of characters used in the phylogenetic analysis

- | | |
|--|---|
| <p>1. Intracranial joint margin:
0. straight
1. strongly interdigitate</p> <p>2. Snout bones:
0. lying free from one another
1. consolidated</p> <p>3. Median rostral:
0. single
1. several median rostrals (internasals)</p> <p>4. Premaxillae:
0. paired
1. fragmented</p> <p>5. Premaxilla:
0. with dorsal lamina
1. without dorsal lamina</p> <p>6. Anterior opening of the rostral organ contained:
0. within premaxilla
1. within separated rostral ossicle</p> <p>7. Parietal:
0. one pair
1. two pairs</p> <p>8. Anterior and posterior pairs of parietals:
0. of similar size
1. of dissimilar size</p> <p>9. Number of supraorbitals/tectals:
0. fewer than eight
1. more than 10</p> <p>10. Preorbital:
0. absent
1. present</p> <p>11. Parietal descending process:
0. absent
1. present</p> <p>12. Intertemporal:
0. absent
1. present</p> <p>13. Postparietal descending process:
0. absent
1. present</p> <p>14. Supratemporal descending process:
0. absent
1. present</p> <p>15. Extrascapulars:
0. sutured with postparietals
1. free</p> <p>16. Extrascapulars:
0. behind level of neurocranium
1. forming part of the skull roof</p> <p>17. Number of extrascapulars:
0. three
1. five
2. more than seven</p> | <p>18. Posterior margin of the skull roof:
0. straight
1. embayed</p> <p>19. Supraorbital sensory canal:
0. running through centre of ossification
1. following sutural course</p> <p>20. Medial branch of otic canal:
0. absent
1. present</p> <p>21. Otic canal:
0. joining supratemporal canal within lateral extrascapular
1. in supratemporal</p> <p>22. Anterior branches of supratemporal commissure:
0. absent
1. present</p> <p>23. Supraorbital sensory canals opening through bones:
0. as single large pores
1. bifurcating pores
2. many tiny pores
3. a large, continuous groove crossed by pillars</p> <p>24. Anterior pit line:
0. absent
1. present</p> <p>25. Middle and posterior pit lines:
0. within posterior half of postparietals
1. within anterior third</p> <p>26. Pit lines:
0. marking postparietals
1. not marking postparietals</p> <p>27. Parietals and postparietals:
0. ornamented with enamel-capped ridges/tubercles
1. bones unornamented
2. bones marked by coarse rugosities</p> <p>28. Parietals and postparietals:
0. without raised areas
1. with raised areas</p> <p>29. Cheek bones :
0. sutured to one another
1. separated from one another</p> <p>30. Spiracular (postspiracular):
0. absent
1. present</p> <p>31. Preoperculum:
0. absent
1. present</p> <p>32. Suboperculum:
0. absent
1. present</p> |
|--|---|

33. **Quadratojugal:**
0. absent
1. present
34. **Squamosal:**
0. limited to the mid-level of cheek
1. extending behind the postorbital to reach the skull roof
35. **Lachrymojugal:**
0. not expanded anteriorly
1. expanded anteriorly
36. **Lachrymojugal:**
0. ending without anterior angle
1. angled anteriorly
37. **Squamosal:**
0. large
1. reduced to a narrow tube surrounding the jugal sensory canal only
38. **Preoperculum:**
0. large
1. reduced to a narrow tube surrounding the preopercular canal only
39. **Preoperculum:**
0. undifferentiated
1. developed as a posterior tube-like canal-bearing portion and an anterior blade-like portion
40. **Postorbital:**
0. simple, without anterodorsal excavation
1. anterodorsal excavation in the postorbital
41. **Postorbital:**
0. without anterior process
1. with anterior process
42. **Postorbital:**
0. large
1. reduced to a narrow tube surrounding the sensory canal only
43. **Postorbital:**
0. entirely behind the level of the intracranial joint
1. spanning the intracranial joint
44. **Infraorbital canal within the postorbital:**
0. with simple pores opening directly from the main canal
1. anterior and posterior branches with the postorbital
45. **Infraorbital sensory canal:**
0. running through centre of postorbital
1. running at the anterior margin of the postorbital
46. **Jugal sensory canal:**
0. simple
1. with prominent branches
47. **Jugal canal:**
0. running through centre of bone
1. running along the ventral margin of the squamosal
48. **Pit lines:**
0. marking cheek bones
1. failing to mark cheek bones
49. **Ornaments upon cheek bones:**
0. absent
1. tube
2. represented as a coarse superficial rugosity
50. **Infraorbital, jugal and preopercular sensory canals:**
0. opening through many tiny pores
1. opening through a few large pores
2. a large, continuous groove crossed by pillars
51. **Lachrymojugal:**
0. sutured to preorbital and lateral rostral
1. lying in a sutural contact with the tectal-supraorbital series
52. **Sclerotic ossicles:**
0. absent
1. present
53. **Retroarticular and articular:**
0. co-ossified
1. separated
54. **Dentary teeth:**
0. fused to the dentary
1. separated from dentary
55. **Number of anterior coronoids:**
0. 0
1. 1
2. 2
3. 3
4. 4
56. **Coronoid:**
0. opposite to the posterior end of dentary not modified
1. modified
57. **Dentary:**
0. simple
1. dentary hook-shaped
58. **Oral pit line:**
0. confined to angular
1. oral pit line reaching forward to the dentary and/or the splenial
59. **Oral pit line:**
0. located at centre of ossification of angular
1. removed from centre of ossification
60. **Subopercular branch of the mandibular sensory canal:**
0. absent
1. present
61. **Dentary sensory pore:**
0. absent
1. present
62. **Ornaments:**
0. ridged

1. granular
63. **Dentary:**
0. with ornament
1. without ornament
64. **Splenic:**
0. with ornament
1. without ornament
65. **Dentary:**
0. without prominent lateral swelling
1. with swelling
66. **Principal coronoid:**
0. lying free
1. sutured to angular
67. **Coronoid fangs:**
0. absent
1. present
68. **Prearticular and/or coronoid teeth:**
0. pointed and smooth
1. rounded and marked with fine striations radiating from the crown
2. pointed and marked with fine striations
69. **Orbitosphenoid and basisphenoid regions:**
0. co-ossified
1. separate
70. **Optic foramen:**
0. enclosed by basisphenoid extending forward
1. lying within separate interorbital ossification or cartilage
71. **Processus connectens:**
0. failing to meet parasphenoid
1. meeting parasphenoid
72. **Basipterygoid process:**
0. absent
1. present
73. **Antotic process:**
0. not covered by parietal descending process
1. covered
74. **Temporal excavation:**
0. lined with bone
1. not lined
75. **Otico-occipital:**
0. solid
1. separated to prootic/opisthotic
76. **Supraoccipital:**
0. absent
1. present
77. **Vestibular fontanelle:**
0. absent
1. present
78. **Buccohypophysial canal:**
0. closed
1. opening through parasphenoid
79. **Parasphenoid:**
0. without ascending laminae anteriorly
1. with ascending laminae
80. **Suprapterygoid process:**
0. absent
1. present
81. **Vomers:**
0. not meeting in the midline
1. meeting medially
82. **Prootic:**
0. without complex suture with the basioccipital
1. with a complex suture
83. **Superficial ophthalmic branch of anterodorsal lateral line nerve:**
0. not piercing antotic process
1. piercing antotic process
84. **Process on braincase for articulation of infrabranchial 1:**
0. absent
1. present
85. **Separate lateral ethmoids:**
0. absent
1. present
86. **Separate basioccipital:**
0. absent
1. present
87. **Dorsum sellae:**
0. small
1. large and constricting entrance to cranial cavity anterior to the intracranial joint
88. **Extracleithrum:**
0. absent
1. present
89. **Anocleithrum:**
0. simple
1. forked
90. **Posterior neural and haemal spines:**
0. abutting one another
1. not abutting
91. **Occipital neural arches:**
0. not expanded
1. expanded
92. **Ossified ribs:**
0. absent
1. present
93. **Diphycercal tail:**
0. absent
1. present
94. **Fin rays:**
0. more numerous than radials
1. equal in number
95. **Fin ray:**
0. branched
1. unbranched
96. **Fin rays in D1:**
0. > 10
1. 8-9
2. < 8
97. **Caudal lobes:**

- 0. symmetrical
- 1. asymmetrical
- 98. D1:**
 - 0. without denticles
 - 1. with denticles
- 99. Paired fin rays:**
 - 0. not expanded
 - 1. expanded
- 100. Pelvics:**
 - 0. abdominal
 - 1. thoracic
- 101. Basal plate of D1:**
 - 0. with smooth ventral margin
 - 1. emarginated and accommodating the tips of adjacent neural spines
- 102. D2 basal support:**
 - 0. simple
 - 1. forked anteriorly
- 103. Median fin rays:**
 - 0. not expanded
 - 1. expanded
- 104. Scale ornament:**
 - 0. not differentiated
 - 1. differentiated
- 105. Lateral line openings in scales:**
 - 0. single
 - 1. multiple
- 106. Scales:**
 - 0. ornament of ridges or tubercles
 - 1. rugose
- 107. Ossified bladder:**
 - 0. absent
 - 1. present
- 108. Pelvic bones of each side:**
 - 0. remain separate
 - 1. fused in midline
- 109. Ventral keel scales:**
 - 0. absent
 - 1. present
- 110. Ventral swelling of the palatoquadrate:**
 - 0. absent
 - 1. present

